Published for SISSA by Springer

Received: *May 19, 2017*
Accepted: *June 28, 2017*
Published: *July 7, 2017*

Wilson loops in unitary matrix models at finite N

Kazumi Okuyama

Department of Physics, Shinshu University,
Matsumoto 390-8621, Japan

E-mail: kazumi@azusa.shinshu-u.ac.jp

Abstract: It is known that the expectation value of Wilson loops in the Gross-Witten-Wadia (GWW) unitary matrix model can be computed exactly at finite N for arbitrary representations. We study the perturbative and non-perturbative corrections of Wilson loops in the $1/N$ expansion, either analytically or numerically using the exact result at finite N. As a by-product of the exact result of Wilson loops, we propose a large N master field of GWW model. This master field has an interesting eigenvalue distribution. We also study the Wilson loops in large representations, called Giant Wilson loops, and comment on the Hagedorn/deconfinement transition of a unitary matrix model with a double trace interaction.

Keywords: 1/N Expansion, Matrix Models

ArXiv ePrint: 1705.06542

https://doi.org/10.1007/JHEP07(2017)030

Contents

JHEP07(2017)030

1 Introduction

Via gauge/string duality, large N 't Hooft expansion of a gauge theory corresponds to the genus expansion of dual string theory. In general, $1/N$ expansion is an asymptotic series and we need to include non-perturbative corrections corresponding to various brane instantons in the bulk string theory. We expect that we recover the exact result of gauge theory at finite N after including such non-perturbative corrections. In other words, the exact result at finite N can be thought of as a non-perturbative completion of the genus expansion. We can also use this relation in the opposite direction: from the exact result at finite N we can read off the information of non-perturbative corrections either analytically or numerically. This strategy was successfully applied to the study of instanton corrections in ABJM theory on S^3 from the exact values of the partition functions [1–3]. It turned out that the non-perturbative corrections in ABJM theory on S^3 has an interesting connection

to the refined topological string on a certain local Calabi-Yau [4]. We hope that by studying exact partition functions of gauge theories or matrix models at finite N, we can reveal interesting physical/mathematical structure of large N expansion for more general cases.

In this paper, we consider the large N expansion of Gross-Witten-Wadia (GWW) model [5, 6] as a simple example. The GWW model is a unitary matrix model with the action $\mathrm{Tr}(U+U^\dagger)$ and it is well-known that this model has a third order phase transition at large N. Near the critical point we can take a double scaling limit [7]; the GWW model in this limit describes a minimal superstring theory [8] and the genus expansion and the non-perturbative corrections are well-studied in this limit. However, somewhat surprisingly, the $1/N$ expansion and non-perturbative corrections in the GWW model in the off-critical regime have not been understood completely, and the study of such corrections from the modern viewpoint of resurgent trans-series was initiated only recently [9]. In [10, 11], the multi-instanton configuration of GWW model was identified as a complex saddle of unitay matrix integral.

The GWW model is a useful testing ground to study the (non)perturbative corrections in the large N expansion since the partition function and the expectation value of Wilson loops in arbitrary representation can be computed exactly at finite N. In this paper, we study the (non)perturbative corrections in GWW model using the exact result at finite N. It is known that the genus expansion of free energy behaves quite differently in the two phases separated by the third order phase transition. In the *gapped* phase where the eigenvalue density has a gap, the free energy receives all genus corrections, while in the *ungapped* phase where the eigenvalue density does not have a gap, the higher genus corrections vanish beyond genus-zero. The ungapped phase is particularly interesting since the instanton correction is directly accessible by simply subtracting the genus-zero part from the exact free energy at finite N. Indeed we find a perfect agreement between the analytic computation of instanton correction and the exact free energy at finite N.

We can study the expectation value of winding Wilson loops $\langle \mathrm{Tr}\, U^k \rangle$ with winding number $k = 1, 2, \cdots$, in a similar manner. In the gapped phase we compare the exact result and the genus expansion of matrix model and find a perfect agreement. In the ungapped phase, $\langle \mathrm{Tr}\, U^k \rangle$ with $k \geq 2$ has no perturbative correction and hence the instanton correction is directly accessible. We determine the coefficient of instanton correction from numerical fitting using the exact result at finite N.

We also consider the so-called Giant Wilson loops in the large (anti)symmetric representation, where the rank of the representation becomes of order N [12–14]. We compute the one-loop correction to the leading large N result of Giant Wilson loops obtained in [12–14], and we find that the matching with the exact result is improved by adding the one-loop correction.

As an interesting by-product of exact result of Wilson loops, we propose a "master field" of GWW model. The exact form of $\langle \mathrm{Tr}\, U \rangle$ in (3.1) and $\langle \det(x-U) \rangle$ in (4.2) suggests that the $N \times N$ matrix $M_0^{-1} M_1$, with M_k defined in (3.2), can be thought of as a master field of GWW model. It turns out that this master field has an interesting distribution of eigenvalues. In particular, we find numerically that in the ungapped phase the eigenvalues of master field are distributed along a contour of constant effective potential, and this contour is located inside the unit circle on a complex plane.

JHEP07(2017)030

As another example, we study the free energy and (Giant) Wilson loops in a unitary matrix model with a double-trace interaction $\mathrm{Tr}\, U\, \mathrm{Tr}\, U^\dagger$, which we call the "adjoint model". This model naturally appears as a truncation of the thermal partition function of $d = 4$ $\mathcal{N} = 4$ super Yang-Mills (SYM) theory on $S^3 \times S^1$ [15]. This model exhibits a Hagedorn/deconfinement transition, which is holographically dual to the Hawking-Page transition on the bulk gravity side [16]. As discussed in [17], we can compute the partition function and Wilson loops in the adjoint model by a certain integral transformation of the GWW model. Using this relation to the GWW model, we study numerically the behavior of partition function and Wilson loops in the adjoint model.

This paper is organized as follows. In section 2 we study the free energy of GWW model. We find that the exact partition function at finite N correctly reproduces the analytic results of the large N expansion of free energy in both gapped phase and the ungapped phase. In section 3 we study the winding Wilson loops $\langle \mathrm{Tr}\, U^k \rangle$ in GWW model. In the gapped phase we find that the exact result at finite N reproduces the analytic result of genus expansion. In the ungapped phase we determine the coefficients of the first non-trivial instanton correction by numerical fitting. In section 4 we propose a master field of GWW model and study its eigenvalue distribution. In the gapped phase eigenvalues of the master field approaches the known distribution in [5, 6] as N becomes large, while in the ungapped phase we find that the eigenvalues of the master field are distributed inside the unit circle. In section 5 using the exact form of the Wilson loops in general representations, we study the connected part of multi-trace expectation values. In section 6 we study the Wilson loops in the k-th (anti)symmetric representation in the limit where $k, N \to \infty$ with k/N fixed. In section 7 we study the adjoint model with a double-trace interaction $\mathrm{Tr}\, U\, \mathrm{Tr}\, U^\dagger$. We consider the free energy, winding Wilson loops, and Giant Wilson loops in the adjoint model, and study the behavior of these quantities under the Hagedorn/deconfinement transition. We conclude in section 8 with some discussions and future directions. In addition, we have four appendices. In appendix A, we review the exact result of the partition function and Wilson loops in GWW model at finite N. In appendix B, we compute the effective potential for a probe eigenvalue in the ungapped phase of GWW model. In appendix C, we study the one-instanton correction in the ungapped phase of GWW model and determine the overall coefficient of instanton correction by matching the result of double-scaling limit. In appendix D, we compute the genus-one resolvent of GWW model in the gapped phase by using the mapping between the unitary matrix model and the hermitian matrix model.

2 Free energy of GWW model

We are interested in the non-perturbative corrections in the large N expansion of the GWW model defined by[1]

$$Z(N, g) = \int_{\mathrm{U}(N)} dU \exp\left[\frac{Ng}{2} \mathrm{Tr}(U + U^\dagger)\right]. \tag{2.3}$$

[1]Note that our convention of coupling constant is different from [9]

$$Z = \int_{\mathrm{U}(N)} dU \exp\left[\frac{1}{2g_s} \mathrm{Tr}(U + U^\dagger)\right], \tag{2.1}$$

JHEP07(2017)030

It is well-known that the partition function of GWW model can be evaluated exactly at finite N [6, 18][2]

$$Z(N,g) = \det\Big[I_{i-j}(Ng)\Big]_{i,j=1,\cdots N}, \tag{2.4}$$

where $I_\nu(x)$ denotes the modified Bessel function of the first kind. As we will see below, we can study perturbative and non-perturbative corrections to the free energy in the large N expansion from the exact result at finite N (2.4).

In the large N limit with fixed g, the free energy admits the genus expansion

$$\log Z(N,g) = \sum_{\ell=0}^{\infty} N^{2-2\ell} F_\ell(g) + F^{(\text{inst})} \tag{2.5}$$

where $F^{(\text{inst})}$ denotes the exponentially suppressed correction

$$F^{(\text{inst})} = \mathcal{O}(e^{-N}). \tag{2.6}$$

As shown in the seminal papers [5, 6] there is a third order phase transition at $g = 1$ and the genus-zero free energy behaves differently below and above the transition point $g = 1$

$$F_0(g) = \begin{cases} \dfrac{g^2}{4}, & (g < 1), \\ g - \dfrac{1}{2}\log g - \dfrac{3}{4}, & (g > 1). \end{cases} \tag{2.7}$$

This third order phase transition is associated with the opening/closing of the gap of the distribution of eigenvalue $e^{\mathrm{i}\theta}$ of unitary matrix U. The eigenvalue density $\rho(\theta)$ has no gap when $g < 1$ (*ungapped phase*) while it has a gap when $g > 1$ (*gapped phase*):

$$\rho(\theta) = \begin{cases} \dfrac{1}{2\pi}(1 + g\cos\theta), & (|\theta| \le \pi, \quad g < 1), \\ \dfrac{g}{\pi}\cos\dfrac{\theta}{2}\sqrt{\dfrac{1}{g} - \sin^2\dfrac{\theta}{2}}, & (|\theta| \le \alpha, \quad g > 1). \end{cases} \tag{2.8}$$

Here α is the end-point of eigenvalue distribution given by

$$\alpha = 2\arcsin(g^{-1/2}). \tag{2.9}$$

In figure 1, we plot the genus-zero free energy in (2.7) and the exact free energy for $N = 100$ and find a nice agreement, as expected.

where the string coupling g_s and the 't Hooft coupling $t = Ng_s$ are related to our coupling g by

$$g_s = \frac{1}{Ng}, \qquad g = \frac{1}{t}. \tag{2.2}$$

[2] See [19] for a review of unitary matrix models.

JHEP07(2017)030

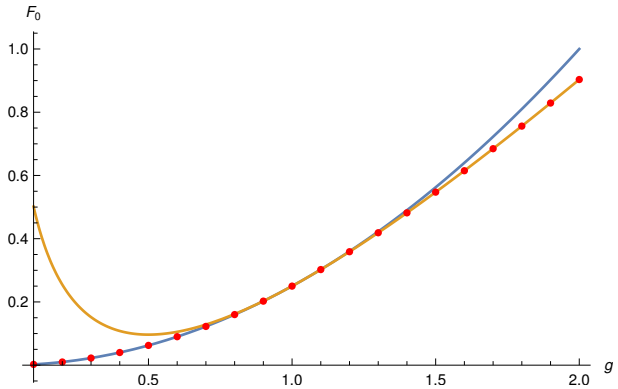

Figure 1. Plot of the genus-zero free energy $F_0(g)$. The red dots are the exact value of the free energy $\frac{1}{N^2}\log Z(N,g)$ for $N=100$, while the blue curve and the orange curve represent the analytic form of $F_0(g)$ in (2.7) in the ungapped phase and the gapped phase, respectively.

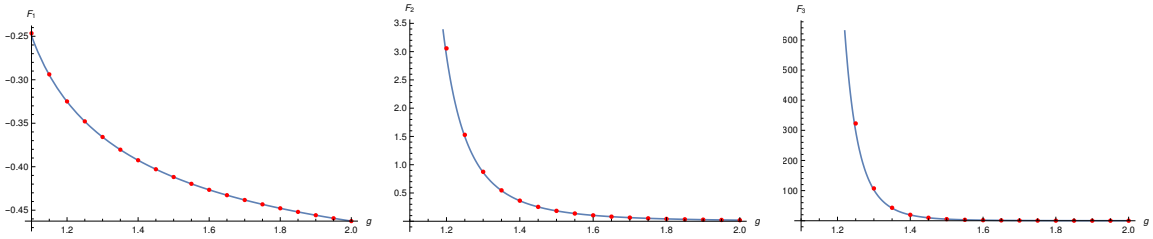

(a) $F_1(g)$. (b) $F_2(g)$. (c) $F_3(g)$.

Figure 2. Plot of the genus-ℓ free energy $F_\ell(g)$ for $\ell=1,2,3$ in the gapped phase ($g>1$). The dots are the values obtained from the exact free energy $\log Z(N,g)$ for $N=100$ using (2.12), while solid curves represent the analytic form of $F_\ell(g)$ in (2.10).

Perturbative corrections in the gapped phase. In the gapped phase ($g>1$), we can systematically compute the genus-ℓ free energy by solving the so-called *pre-string* equation obtained from the method of orthogonal polynomials [7, 9, 20]. The first three terms are given by

$$\begin{aligned} F_1(g) &= \zeta'(-1) - \frac{1}{12}\log N - \frac{1}{8}\log(1-1/g), \\ F_2(g) &= -\frac{1}{240} + \frac{3}{128(g-1)^3}, \\ F_3(g) &= \frac{1}{1008} + \frac{9(5g+2)}{1024(g-1)^6}. \end{aligned} \tag{2.10}$$

In general, the genus ℓ free energy $F_\ell(g)$ has a structure

$$F_\ell(g) = \frac{B_{2\ell}}{2\ell(2\ell-2)} + \frac{1}{(g-1)^{3\ell-3}}\sum_{n=0}^{\ell-2} c_n^{(\ell)} g^n \tag{2.11}$$

where $B_{2\ell}$ denotes the Bernoulli number which comes from the volume of $\mathrm{U}(N)$ gauge group.

JHEP07(2017)030

One can extract the genus-ℓ free energy from the exact value of $Z(N,g)$ in (2.4) by subtracting the lower genus contributions

$$F_\ell(g) \approx N^{2\ell-2}\left(\log Z(N,g) - \sum_{\ell'=0}^{\ell-1} N^{2-2\ell'} F_{\ell'}(g)\right), \quad (N \gg 1). \tag{2.12}$$

As we can see from figure 2, the exact partition function (2.4) nicely matches the analytic result of genus-ℓ free energy (2.10) as expected.

The instanton correction in the gapped phase has been studied in [9]. The genus expansion in the gapped phase is Borel non-summable and in order to compare with the exact result at finite N we need to add the lateral Borel resummations along the integration contours below and above the real axis. On the other hand, in the ungapped phase the perturbative genus expansion stops at first order and we do not need to perform the Borel resummation of perturbative part. As a consequence, in the ungapped phase we can directly access to the instanton correction from the exact result at finite N, as we will see below.

Instanton correction in the ungapped phase. In the ungapped phase ($g < 1$), the genus expansion of free energy stops at genus-zero

$$F_0(g) = \frac{g^2}{4}, \qquad F_\ell(g) = 0 \quad (\ell \geq 1), \tag{2.13}$$

and the instanton correction starts from the two-instanton correction[3]

$$F^{(\text{inst})} = e^{-2NS_{\text{inst}}(g)} \sum_{n=1}^{\infty} \frac{f_n(g)}{N^n} + \mathcal{O}(e^{-4NS_{\text{inst}}(g)}), \tag{2.14}$$

where the instanton action is given by [21, 22]

$$S_{\text{inst}}(g) = \cosh^{-1}(1/g) - \sqrt{1-g^2}. \tag{2.15}$$

One can extract the instanton action numerically from the exact partition function $Z(N,g)$ by subtracting the perturbative part

$$S_{\text{inst}}(g) \approx -\frac{1}{2N}\log\left|\log Z(N,g) - N^2 F_0(g)\right|, \qquad (N \gg 1) \tag{2.16}$$

As shown in figure 3, the exact $Z(N,g)$ correctly reproduces the analytic result of instanton action (2.15).

As explained in appendix C, we can systematically compute the instanton coefficient f_n in (2.14)

$$F^{(2\text{-inst})} = \frac{e^{-2NS_{\text{inst}}(g)}}{8\pi N}\left[-\frac{g^2}{(1-g^2)^{\frac{3}{2}}} + \frac{1}{N}\frac{g^2(26+9g^2)}{12(1-g^2)^3} - \frac{1}{N^2}\frac{g^2(297g^4+2484g^2+964)}{288(1-g^2)^{\frac{9}{2}}} + \cdots\right] \tag{2.17}$$

Instanton coefficient in the ungapped phase has been studied in [9] but the overall factor was not determined in [9]. We have fixed the overall factor ($1/8\pi N$ in (2.17)) by matching the Hastings-McLeod solution of Painlevé II equation in the double scaling limit (see appendix C for details). Also, we have checked numerically that the instanton correction (2.17) to the free energy correctly reproduces the exact value of $\log Z(N,g) - N^2 F_0(g)$.

[3] As explained in appendix C, the expectation value of $\det U$ receives one-instanton correction $\mathcal{O}(e^{-NS_{\text{inst}}(g)})$, while the instanton correction to the free energy starts from the two-instanton $\mathcal{O}(e^{-2NS_{\text{inst}}(g)})$.

JHEP07(2017)030

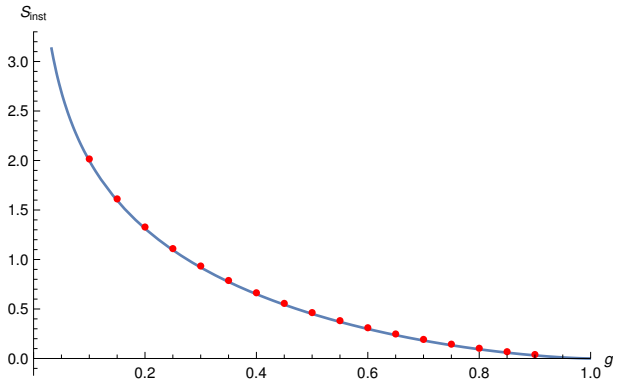

Figure 3. Plot of the instanton action $S_{\text{inst}}(g)$ in the range $0 < g < 1$. The red dots are the numerical values extracted from the exact free energy using (2.16) with $N = 400$, while the solid curve represent the analytic form of $S_{\text{inst}}(g)$ in (2.15).

3 Winding Wilson loops

In this section, we consider the expectation value of winding Wilson loop $\langle \operatorname{Tr} U^k \rangle$ with winding number $k \in \mathbb{Z}_{>0}$. One can show that $\langle \operatorname{Tr} U^k \rangle$ can be computed exactly at finite N (see appendix A for a derivation)

$$\langle \operatorname{Tr} U^k \rangle = \operatorname{Tr}(M_0^{-1} M_k), \tag{3.1}$$

where M_k is an $N \times N$ matrix whose (i, j) element is given by

$$(M_k)_{i,j} = I_{k+i-j}(Ng), \qquad (i, j = 1, \cdots, N). \tag{3.2}$$

For $k = 1$ the expectation value is related to the derivative of free energy

$$\frac{1}{N} \langle \operatorname{Tr} U \rangle = \frac{1}{N^2} \partial_g \log Z(N, g). \tag{3.3}$$

In the planar limit we find

$$\frac{1}{N} \langle \operatorname{Tr} U \rangle = \partial_g F_0(g) = \begin{cases} \dfrac{g}{2}, & (g < 1), \\ 1 - \dfrac{1}{2g}, & (g > 1). \end{cases} \tag{3.4}$$

For $k \geq 2$ the expectation value in the planar limit is obtained using the eigenvalue density (2.8) as

$$\frac{1}{N} \langle \operatorname{Tr} U^k \rangle = \int d\theta \rho(\theta) e^{\mathrm{i}k\theta} = \begin{cases} 0, & (g < 1), \\ \dfrac{1}{k-1} \left(1 - \dfrac{1}{g}\right)^2 P_{k-2}^{(1,2)} \left(1 - \dfrac{2}{g}\right), & (g > 1), \end{cases} \tag{3.5}$$

where $P_n^{(\alpha,\beta)}(x)$ denotes the Jacobi polynomial.

Again, we can compare the analytic expression of $\frac{1}{N} \langle \operatorname{Tr} U^k \rangle$ in the planar limit (3.5) and the exact value at finite N (3.1). In figure 4 and figure 5, we show the plot of $\frac{1}{N} \langle \operatorname{Tr} U^k \rangle$ for $k = 1, 2, 3, 4$. We find perfect agreement between the analytic result and the exact value at finite N, as expected.

JHEP07(2017)030

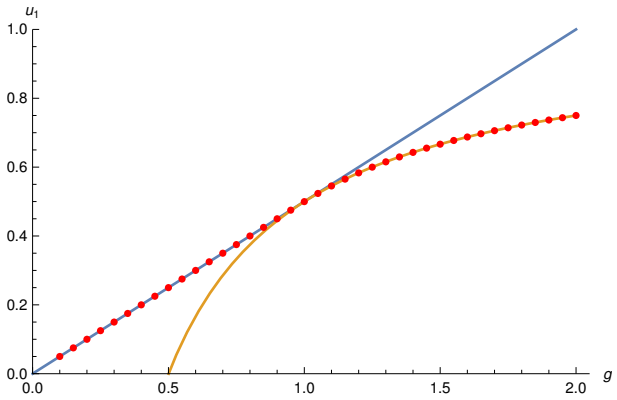

Figure 4. Plot of the expectation value of Wilson loop $u_1 = \frac{1}{N}\langle \mathrm{Tr}\, U\rangle$. The red dots are the exact value for $N = 100$, while the blue curve and the orange curve are the planar limit (3.4) in the ungapped phase and the gapped phase, respectively.

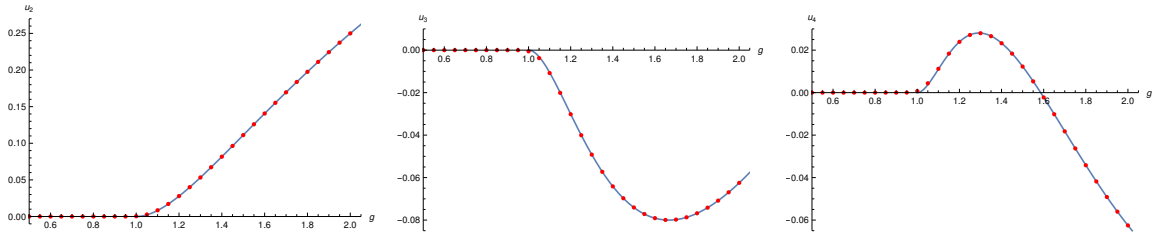

(a) u_2. (b) u_3. (c) u_4.

Figure 5. Plot of the expectation value of the winding Wilson loops $u_k = \frac{1}{N}\langle \mathrm{Tr}\, U^k\rangle$ for $k = 2, 3, 4$. The red dots are the exact values at $N = 100$, while solid curves represent the planar limit in (3.5).

Genus expansion in the gapped phase. From the exact value of winding Wilson loops at finite N (3.1), one can determine the higher genus correction to the winding Wilson loops by numerical fitting. In the gapped phase, winding Wilson loops receives all-order corrections in the $1/N$ expansion. For winding numbers $k = 1, \cdots, 5$, we find numerically the genus expansion in the gapped phase:

$$
\begin{aligned}
\frac{1}{N}\langle \mathrm{Tr}\, U\rangle &= 1 - \frac{1}{2g} - \frac{1}{N^2}\frac{1}{8(g-1)g} - \frac{1}{N^4}\frac{9}{128(g-1)^4} - \frac{1}{N^6}\frac{9(25g+17)}{1024(g-1)^7} + \cdots, \qquad (3.6)\\
\frac{1}{N}\langle \mathrm{Tr}\, U^2\rangle &= \frac{(g-1)^2}{g^2} + \frac{1}{N^2}\frac{1}{4(g-1)g^2} + \frac{1}{N^4}\frac{9}{64(g-1)^4 g} + \frac{1}{N^6}\frac{451g^2+297g+23}{1024(g-1)^7 g^2} + \cdots,\\
\frac{1}{N}\langle \mathrm{Tr}\, U^3\rangle &= \frac{(g-1)^2(2g-5)}{2g^3} + \frac{1}{N^2}\frac{10-28g+15g^2}{8(g-1)g^3} + \frac{1}{N^4}\frac{3(20-90g+96g^2-35g^3)}{128(g-1)^4 g^3} + \cdots,\\
\frac{1}{N}\langle \mathrm{Tr}\, U^4\rangle &= \frac{(g-1)^2\left(g^2-6g+7\right)}{g^4} + \frac{1}{N^2}\frac{-35+90g-70g^2+16g^3}{2(g-1)g^4}\\
&\quad + \frac{1}{N^4}\frac{-154+561g-624g^2+226g^3}{32(g-1)^4 g^4} + \cdots,
\end{aligned}
$$

JHEP07(2017)030

$$\frac{1}{N}\langle \mathrm{Tr}\, U^5\rangle = \frac{(g-1)^2\left(2g^3-21g^2+56g-42\right)}{2g^5}+\frac{1}{N^2}\frac{5\left(35g^4-260g^3+630g^2-616g+210\right)}{8(g-1)g^5} + \frac{1}{N^4}\frac{26460g^5-130688g^4+241751g^3-209326g^2+84392g-12772}{512(g-1)^4g^5}+\cdots .$$

The planar part of (3.6) agrees with (3.4) for $k=1$ and (3.5) for $k\geq 2$. One can in principle compute the higher genus corrections of winding Wilson loops analytically and compare our numerical result (3.6). For instance, the genus-one resolvent can be easily found by mapping the unitary matrix model to ordinary Hermitian matrix model by a change of variable [23]. As explained in appendix D, we have checked that the genus-one correction in (3.6) is correctly reproduced from the analytic form of the genus-one resolvent. It would be interesting to analytically compute the higher genus corrections to the winding Wilson loops and compare our numerical result (3.6).

Instanton correction in the ungapped phase. In the ungapped phase ($g<1$), the perturbative $1/N$ correction to the winding Wilson loops stops at the first few orders. For $k=1$, the instanton correction is readily obtained by taking the derivative of free energy with respect to g (3.3)

$$\frac{1}{N}\langle \mathrm{Tr}\, U\rangle - \frac{g}{2} = \frac{e^{-2NS_{\mathrm{inst}}(g)}}{4\pi N^2}\left[\frac{-g}{1-g^2}+\frac{1}{N}\frac{g(14+3g^2)}{12(1-g^2)^{\frac{5}{2}}}-\frac{1}{N^2}\frac{g(340+804g^2+81g^4)}{288(1-g^2)^4}+\mathcal{O}(N^{-3})\right]. \tag{3.7}$$

For $k\geq 2$, there is no perturbative piece and the non-zero contribution starts from the two-instanton correction. From the exact value of $\langle \mathrm{Tr}\, U^k\rangle$ in (3.1), we can determine the instanton coefficients numerically. Although we do not know *a priori* the analytic structure of the instanton coefficients in $\langle \mathrm{Tr}\, U^k\rangle$ for $k\geq 2$, it is natural to expect that the instanton correction for $k\geq 2$ is similar to that of $k=1$ in (3.7). Then we can make an ansatz similar to (3.7) and fix the coefficients by numerical fitting assuming that the unknown coefficients are rational numbers. In this way we find

$$\begin{aligned}
\frac{1}{N}\langle \mathrm{Tr}\, U^2\rangle &= \frac{e^{-2NS_{\mathrm{inst}}(g)}}{4\pi N^2}\left[\frac{2}{1-g^2}-\frac{1}{N}\frac{28+5g^2}{12(1-g^2)^{\frac{5}{2}}}+\mathcal{O}(N^{-2})\right],\\
\frac{1}{N}\langle \mathrm{Tr}\, U^3\rangle &= \frac{e^{-2NS_{\mathrm{inst}}(g)}}{4\pi N^2}\left[\frac{-4+g^2}{(1-g^2)g}+\mathcal{O}(N^{-1})\right],\\
\frac{1}{N}\langle \mathrm{Tr}\, U^4\rangle &= \frac{e^{-2NS_{\mathrm{inst}}(g)}}{4\pi N^2}\left[\frac{8-4g^2}{(1-g^2)g^2}+\mathcal{O}(N^{-1})\right].
\end{aligned} \tag{3.8}$$

As far as we know, no systematic method to compute instanton corrections for general Wilson loops is known in the literature. It would be interesting to develop a technique to compute instanton corrections to the Wilson loops and see if our numerical results (3.8) are reproduced.

4 Master field of GWW model and its eigenvalue distribution

In this section we propose a "master field" of GWW model and study its eigenvalue distribution.

JHEP07(2017)030

Master field of GWW model. From the relation $\langle \mathrm{Tr}\, U \rangle = \mathrm{Tr}(M_0^{-1} M_1)$ in (3.1), it is natural to conjecture that the $N \times N$ matrix $M_0^{-1} M_1$ can be thought of as a "master field" of GWW model

$$U \;\leftrightarrow\; M_0^{-1} M_1. \tag{4.1}$$

In fact, we can prove more general correspondence: expectation value of the characteristic polynomial of U is given by the characteristic polynomial of master field (see appendix A)

$$\langle \det(x - U) \rangle = \det(x - M_0^{-1} M_1). \tag{4.2}$$

Moreover, we have checked numerically that the expectation values of winding Wilson loops are also reproduced from the trace of master field in the large N limit

$$\langle \mathrm{Tr}\, U^k \rangle = \mathrm{Tr}(M_0^{-1} M_1)^k, \qquad (N \gg 1). \tag{4.3}$$

Note that for $k = 1$ the relation (4.3) is exact at finite N, while for $k \geq 2$ this relation (4.3) holds only in the planar limit.

From the explicit form of the matrix M_k (3.2), One can easily show that the master field $M_0^{-1} M_1$ has the form[4]

$$M_0^{-1} M_1 = \begin{pmatrix} a_1 & 1 & 0 & \dots & 0 \\ a_2 & 0 & 1 & \dots & 0 \\ \vdots & & & \ddots & \vdots \\ a_{N-1} & 0 & 0 & \dots & 1 \\ a_N & 0 & 0 & \dots & 0 \end{pmatrix}, \tag{4.4}$$

where a_i appears as the coefficient of characteristic polynomial

$$\langle \det(x - U) \rangle = x^N - \sum_{i=1}^{N} a_i x^{N-i}. \tag{4.5}$$

In other words, a_i is the expectation value of Wilson loops in the i-th anti-symmetric representation up to a sign $(-1)^{i-1}$.

Eigenvalue distribution of master field. It is interesting to consider the eigenvalue distribution of the master field for large but finite N and compare it with the known planar eigenvalue distribution of GWW model. First of all, the master field $M_0^{-1} M_1$ is not a unitary matrix at finite N, hence it is not clear whether such a comparison is meaningful. Nevertheless, we find numerically that in the gapped phase the eigenvalues of $M_0^{-1} M_1$ approaches the large N distribution $\rho(\theta)$ in (2.8) on the unit circle as N becomes large (see figure 6).

On the other hand, in the ungapped phase the eigenvalues of master field are distributed inside the unit circle (see figure 7). Interestingly, those eigenvalues are distributed along a constant potential contour $\Phi(z) = -S_{\mathrm{inst}}(g)$ on the complex z-plane, where $S_{\mathrm{inst}}(g)$

[4]We would like to thank Pavel Buividovich for pointing out this structure.

JHEP07(2017)030

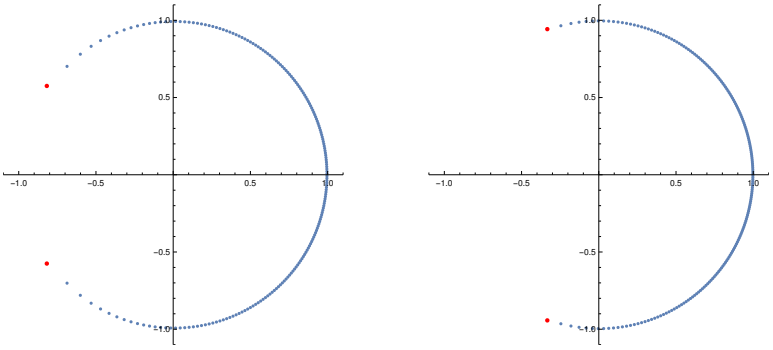

(a) $g = 1.1$. (b) $g = 1.5$.

Figure 6. Plot of the eigenvalues of the matrix $M_0^{-1}M_1$ for $N = 200$ at (a) $g = 1.1$ and (b) $g = 1.5$. The red dots represent the end-point $e^{\pm i\alpha}$ of the cut in the large N limit.

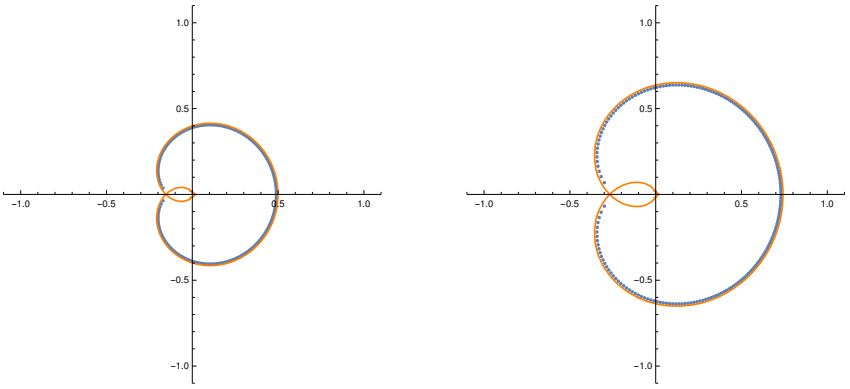

(a) $g = 0.3$. (b) $g = 0.5$.

Figure 7. Plot of the eigenvalues of the matrix $M_0^{-1}M_1$ for $N = 200$ at (a) $g = 0.3$ and (b) $g = 0.5$. The dots are the eigenvalues of matrix $M_0^{-1}M_1$, while the orange curves represent the equi-potential contour $\Phi(z) = -S_{\rm inst}(g)$.

is the instanton action in the ungapped phase (2.15) and the effective potential $\Phi(z)$ for the probe eigenvalue is given by (see appendix B)

$$\Phi(z) = \begin{cases} -\mathrm{Re}\left[\dfrac{g}{2}(z - z^{-1}) + \log z\right], & (|z| > 1), \\ \mathrm{Re}\left[\dfrac{g}{2}(z - z^{-1}) + \log z\right], & (|z| < 1). \end{cases} \tag{4.6}$$

One can show that, in analogy with an electrostatic problem, in the large N limit the eigenvalues are distributed along the loci of constant effective potential.

As shown in figure 8, this potential has minimum at $z = z_\pm$ on the negative real z-axis

$$z_\pm = \frac{-1 \pm \sqrt{1 - g^2}}{g}, \tag{4.7}$$

and the values of the potential at $z = z_\pm$ and $z = -1$ are found to be

$$\Phi(z_\pm) = -S_{\rm inst}(g), \quad \Phi(-1) = 0. \tag{4.8}$$

JHEP07(2017)030

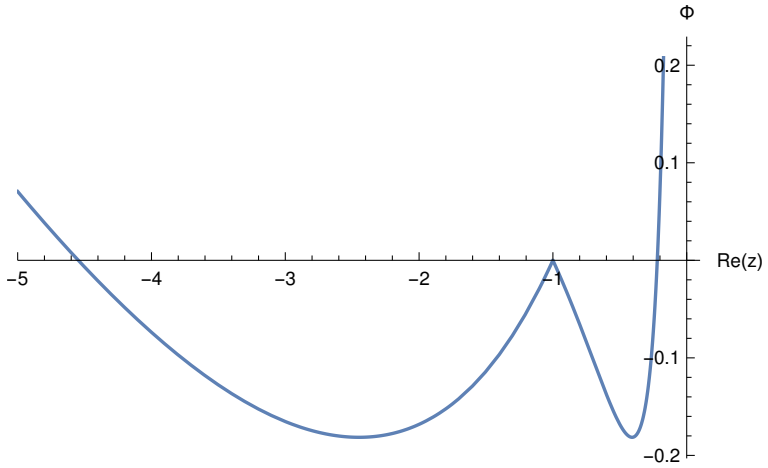

Figure 8. Effective potential $\Phi(z)$ along the negative real z-axis for $g = 0.7$.

Note that the potential is constant along the unit circle

$$\Phi(z) = 0 \quad \text{for} \quad |z| = 1, \tag{4.9}$$

and this is *higher* than the potential at $z = z_\pm$ (4.8).[5] This seems to suggest that the eigenvalue distribution along the contour $\Phi(z) = -S_{\text{inst}}(g)$ is more stable than the distribution along the unit circle.

It is tempting to identify the one-instanton correction $\mathcal{O}(e^{-NS_{\text{inst}}(g)})$ as the effect of eigenvalue tunneling from $z = z_-$ to $z = -1$. However, it is not clear to us whether the eigenvalue distribution along the contour $\Phi(z) = -S_{\text{inst}}(g)$ is realized as a complex saddle of the GWW matrix integral.[6] It would be very interesting to clarify this point further.

5 Wilson loops in various representations

We can compute the expectation value of Wilson loops in general representation exactly at finite N. One can show that the expectation value of the Wilson loop labeled by a Young diagram λ is given by (see appendix A)

$$\langle \mathrm{Tr}_\lambda U \rangle = \frac{\det\left[I_{\lambda_j+i-j}(Ng)\right]}{\det\left[I_{i-j}(Ng)\right]}. \tag{5.1}$$

In this section we consider Wilson loops in "small representations" where the number of boxes in the corresponding Young diagram is small compared to N. For small representations, it is convenient to use multi-trace basis rather than irreducible representations since the connected part of multi-trace expectation value has a well-defined $1/N$ expansion in

[5] This is different from the claim in [11]. In our notation, eq. (89) in [11] reads $\Phi(z_\pm) = +S_{\text{inst}}(g)$, but we believe that eq. (89) in [11] has a sign error.

[6] We would like to thank P. Buividovich, G. Dunne, and S. Valgushev for discussion on this point.

JHEP07(2017)030

the gapped phase

$$\left\langle \prod_{i=1}^{h} \mathrm{Tr}\, U^{k_i} \right\rangle_{\mathrm{conn}} = \sum_{\ell=0}^{\infty} N^{2-2\ell-h} W_\ell(k_1, \cdots, k_h). \tag{5.2}$$

In the next section, we will consider Wilson loops in large representations.

For instance, using the relations

$$\begin{aligned} (\mathrm{Tr}\, U)^2 &= \ydiagram{2} \ + \ydiagram{1,1} \ , \\ \mathrm{Tr}\, U\, \mathrm{Tr}\, U^2 &= \ydiagram{3} \ - \ydiagram{2,1} \ , \\ (\mathrm{Tr}\, U)^3 &= \ydiagram{3} \ + \ydiagram{2,1} \ + 2\ydiagram{2,2} \ , \end{aligned} \tag{5.3}$$

we can compute the expectation values of the left-hand-side of (5.3) by a combination of (5.1) and find the (non)perturbative corrections numerically. As in the case of winding Wilson loops considered in section 3, we do not know the analytic structure of such corrections *a priori*, but we can make an appropriate ansatz similar to the known results of free energy and $\langle \mathrm{Tr} U \rangle$, and fix the unknown coefficients by numerical fitting. In this manner we find the genus expansion in the gapped phase

$$\begin{aligned} \langle (\mathrm{Tr}\, U)^2 \rangle_{\mathrm{conn}} &= -\frac{g-1}{g^2} + \frac{1}{N^2} \frac{-2+3g}{8(g-1)^2 g^2} + \cdots , \\ \langle \mathrm{Tr}\, U\, \mathrm{Tr}\, U^2 \rangle_{\mathrm{conn}} &= -\frac{2(g-1)(g-2)}{g^3} + \frac{1}{N^2} \frac{4-5g}{4(g-1)^2 g^3} + \cdots , \\ \langle (\mathrm{Tr}\, U)^3 \rangle_{\mathrm{conn}} &= \frac{1}{N} \frac{-4+3g}{g^3} + \frac{1}{N^3} \frac{-8+21g-15g^2}{8(g-1)^3 g^3} + \cdots , \end{aligned} \tag{5.4}$$

while in the ungapped phase we find the leading non-trivial instanton coefficients

$$\begin{aligned} \langle (\mathrm{Tr}\, U)^2 \rangle_{\mathrm{conn}} &= \frac{e^{-2N S_{\mathrm{inst}}(g)}}{4\pi N} \left[\frac{-2}{\sqrt{1-g^2}} + \mathcal{O}(N^{-1}) \right] , \\ \langle \mathrm{Tr}\, U\, \mathrm{Tr}\, U^2 \rangle_{\mathrm{conn}} &= \frac{e^{-2N S_{\mathrm{inst}}(g)}}{4\pi N} \left[\frac{4}{g\sqrt{1-g^2}} + \mathcal{O}(N^{-1}) \right] , \\ \langle (\mathrm{Tr}\, U)^3 \rangle_{\mathrm{conn}} &= \frac{e^{-2N S_{\mathrm{inst}}(g)}}{4\pi N} \left[\frac{-4}{g} + \mathcal{O}(N^{-1}) \right] . \end{aligned} \tag{5.5}$$

It is would be interesting to compute the genus expansion analytically in the gapped phase (5.4) by using the relation between unitary matrix model and hermitian matrix model as discussed in appendix D.

6 Giant Wilson loops

In this section we consider Wilson loops in large representations, which are also dubbed "Giant Wilson loops". In $d = 4$ $\mathcal{N} = 4$ SYM, Giant Wilson loops are particularly interesting since they are holographically dual to some D-brane configurations in $AdS_5 \times S^5$ [24–26]. In [12–14], Giant Wilson loops in unitary matrix models were studied in the large N limit.

JHEP07(2017)030

For large symmetric representation, it was found that the there is a first order phase transition as we increase the rank of representation.

In this section, we consider the one-loop correction to the Giant Wilson loops in GWW model in the $1/N$ expansion and find a perfect match with the exact finite N result.

6.1 Symmetric representation

In this subsection, we consider the Wilson loops $W_{S_k} = \langle \mathrm{Tr}_{S_k} U \rangle$ in the k-th symmetric representation S_k. We are interested in the regime where k scales as N with the ratio $x = k/N$ fixed

$$k, N \to \infty, \qquad x = \frac{k}{N} : \text{ fixed}. \tag{6.1}$$

It is convenient to consider the generating function of W_{S_k}

$$e^{NF_S(t)} \equiv \sum_{k=0}^{\infty} t^k W_{S_k} = \langle \det(1 - tU)^{-1} \rangle, \tag{6.2}$$

and W_{S_k} is extracted by

$$W_{S_k} = \oint_{t=0} \frac{dt}{2\pi \mathrm{i} t^{k+1}} e^{NF_S(t)}. \tag{6.3}$$

In the large N limit, $F_S(t)$ is given by the integral with the eigenvalue density $\rho(\theta)$ in (2.8) as a weight

$$F_S(t) = -\int d\theta \rho(\theta) \log(1 - te^{\mathrm{i}\theta}). \tag{6.4}$$

Gapped phase. Let us consider the generating function $F_S(t)$ (6.4) in the gapped phase. As shown in [13], the derivative of $F_S(t)$ in the planar limit can be written in a closed form

$$t\partial_t F_S = \int d\theta \rho(\theta) \frac{te^{\mathrm{i}\theta}}{1 - te^{\mathrm{i}\theta}} = -\frac{1}{2} + \frac{g(t+1)}{4t} \left[t - 1 + \sqrt{(t-1)^2 + \frac{4t}{g}} \right]. \tag{6.5}$$

In the limit (6.1), the integral (6.3) can be evaluated by the saddle point approximation, where the saddle point equation reads

$$t\partial_t F_S = x, \tag{6.6}$$

and the solution of saddle point equation is given by

$$t_* = \frac{(1+2x)^2 - 2g + (1+2x)\sqrt{(1+2x)^2 + 4g(g-1)}}{4g(1+x)}. \tag{6.7}$$

The saddle point value is evaluated as

$$\begin{aligned} F_S(t_*) - x \log t_* = {} & \frac{1}{2}\left(1 - 2g + \sqrt{(1+2x)^2 + 4g(g-1)}\right) \\ & + \log \frac{1 + 2x + 2g - \sqrt{(1+2x)^2 + 4g(g-1)}}{2} - x \log t_*. \end{aligned} \tag{6.8}$$

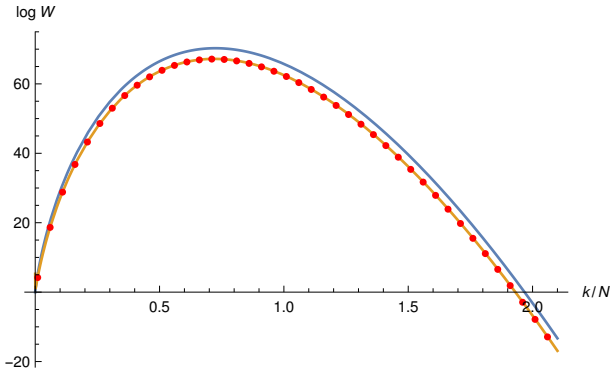

Figure 9. Plot of $\log W_{S_k}$ in the gapped phase ($g = 1.5, N = 100$). The red dots are the exact values, while the blue curve and the orange curve represent the leading term and the leading+one-loop correction in (6.9), respectively. One can see that the one-loop correction improves the matching with the exact result.

One can also compute the one-loop correction from the Gaussian fluctuation around the saddle point. At this order we do not need the genus-one correction to $\rho(\theta)$. Finally, we find

$$\log W_{S_k} = N\Big[F_S(t_*) - x\log t_*\Big] - \frac{1}{2}\log\Big[2\pi N F_S''(t_*)\Big], \tag{6.9}$$

where $F_S''(t_*)$ denotes the second derivative of F_S with respect to $\log t$

$$F_S''(t_*) = \frac{(1+2x)^2 + 2(g-1) - \sqrt{(1+2x)^2+4g(g-1)}}{2(1+2x)^2+8(g-1)}\sqrt{(1+2x)^2+4g(g-1)}. \tag{6.10}$$

In figure 9, we show the plot of $\log W_{S_k}$ as a function of $x = k/N$ for $g = 1.5$. One can see that including the one-loop correction (i.e. the second term in (6.9)) improves the matching with the exact value of $\log W_{S_k}$ at finite N.

Ungapped phase. In the ungapped phase, W_{S_k} is dominated by the $\langle \mathrm{Tr}\, U\rangle^k$ term since higher traces $\mathrm{Tr}\, U^m$ $(m \geq 2)$ are exponentially suppressed in the large N limit [12]

$$W_{S_k} \approx \frac{1}{k!}\langle \mathrm{Tr}\, U\rangle^k \approx \frac{1}{k!}\left(\frac{Ng}{2}\right)^k. \tag{6.11}$$

Using the Stirling's formula

$$k! \approx \sqrt{2\pi N x}\left(\frac{Nx}{e}\right)^{Nx}, \tag{6.12}$$

we find

$$\log W_{S_k} = Nx\log\left(\frac{eg}{2x}\right) - \frac{1}{2}\log(2\pi N x). \tag{6.13}$$

The second term can be thought of as the "one-loop" correction to the result in [12]. Again, as shown in figure 10, the one-loop correction improves the matching with the exact result at finite N.

JHEP07(2017)030

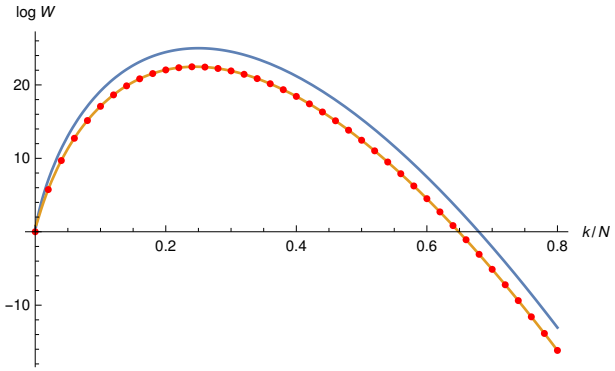

Figure 10. Plot of $\log W_{S_k}$ in the ungapped phase ($g = 0.5, N = 100$). The red dots are the exact values, while the blue curve and the orange curve represent the leading term and the leading+one-loop correction in (6.13), respectively. Again, one can see that the inclusion of the one-loop correction improves the matching.

6.2 Anti-symmetric representation

In this section we consider the Wilson loops $W_{A_k} = \langle \mathrm{Tr}_{A_k} U \rangle$ of GWW model in the k-th anti-symmetric representation A_k in the limit (6.1). As in the case of symmetric representation, it is convenient to consider the generating function of W_{A_k}

$$e^{NF_A(t)} \equiv \sum_{k=0}^{N} t^k W_{A_k} = \langle \det(1+tU) \rangle. \tag{6.14}$$

In the large N limit, $F_A(t)$ is given by an integral with weight $\rho(\theta)$

$$F_A(t) = \int d\theta \rho(\theta) \log(1 + te^{\mathrm{i}\theta}) \tag{6.15}$$

and the W_{A_k} is given by

$$W_{A_k} = \oint \frac{dt}{2\pi \mathrm{i} t^{k+1}} e^{NF_A(t)}. \tag{6.16}$$

Gapped phase. Let us consider W_{A_k} in the gapped phase. Again, in the limit (6.1) the integral (6.16) can be evaluated by the saddle point approximation. The saddle point equation is

$$t\partial_t F_A = x, \tag{6.17}$$

where the left-hand-side is computed as

$$t\partial_t F_A = \int d\theta \rho(\theta) \frac{te^{\mathrm{i}\theta}}{1+te^{\mathrm{i}\theta}} = \frac{1}{2} + \frac{g(t-1)}{4t}\left[t+1-\sqrt{(t+1)^2 - \frac{4t}{g}}\right]. \tag{6.18}$$

There are two solutions of saddle point equation, but the solution corresponding to the dominant saddle turns out to be [14]

$$t_* = \frac{2g - (1-2x)^2 - (1-2x)\sqrt{(1-2x)^2 - 4g(1-g)}}{4g(1-x)}, \tag{6.19}$$

JHEP07(2017)030

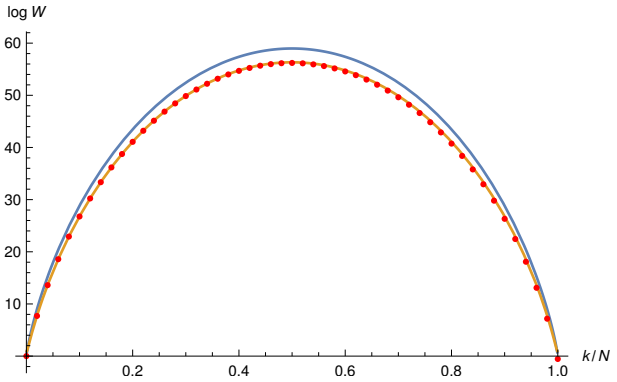

Figure 11. Plot of the log of Wilson loop in the anti-symmetric representation $\log W_{A_k}$ as a function of k/N for $g = 1.5, N = 100$. The red dots are the exact values while the blue curve and the orange curve are the leading term and the leading+one-loop correction in (6.21), respectively. One can clearly see that the inclusion of the one-loop correction improves the matching with the exact value.

and the saddle point value is

$$\begin{aligned} F_A(t_*) - x\log t_* = &\frac{1}{2}\Big(2g - 1 - \sqrt{(1-2x)^2 - 4g(1-g)}\Big) \\ &+ \frac{1}{2}\log\frac{2g - 1 + \sqrt{(1-2x)^2 - 4g(1-g)}}{4gx(1-x)} \\ &- \frac{x}{2}\log t_*(x) - \frac{1-x}{2}\log t_*(1-x). \end{aligned} \tag{6.20}$$

Note that (6.20) is symmetric under the exchange $x \leftrightarrow 1-x$. One can also compute the one-loop correction by performing the Gaussian integral around the saddle point

$$\log W_{A_k} = N\Big[F_A(t_*) - x\log t_*\Big] - \frac{1}{2}\log\Big[2\pi N F_A''(t_*)\Big], \tag{6.21}$$

where

$$F_A''(t_*) = \frac{(1-2x)^2 + 2(g-1) + \sqrt{(1-2x)^2 - 4g(1-g)}}{2(1-2x)^2 + 8(g-1)}\sqrt{(1-2x)^2 - 4g(1-g)}. \tag{6.22}$$

As one can see from figure 11, matching with the exact value at finite N is improved by including the one-loop correction.

Ungapped phase. In [13], it was found that in the ungapped phase the symmetry $k \to N-k$ of W_{A_k} is realized by a first order phase transition for the model with gauge group SU(N). In our case of U(N) matrix model, there is no such symmetry at finite N, although we have an approximate symmetry $k \to N-k$ in the gapped phase in the large N limit (see figure 11). As shown in figure 12, we indeed find that the W_{A_k} is not symmetric under $k \to N-k$ in the ungapped phase. It would be interesting to find the exact form of W_{A_k} for SU(N) theory at finite N and confirm the result of [13].

JHEP07(2017)030

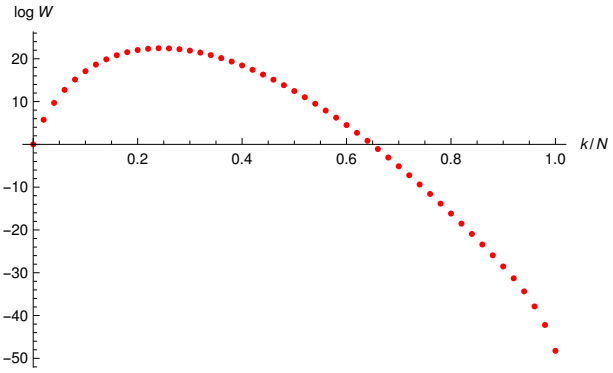

Figure 12. Plot of $\log W_{A_k}$ in the ungapped phase ($g = 0.5, N = 100$). We do not have a symmetry $k \leftrightarrow N - k$ in the U(N) theory.

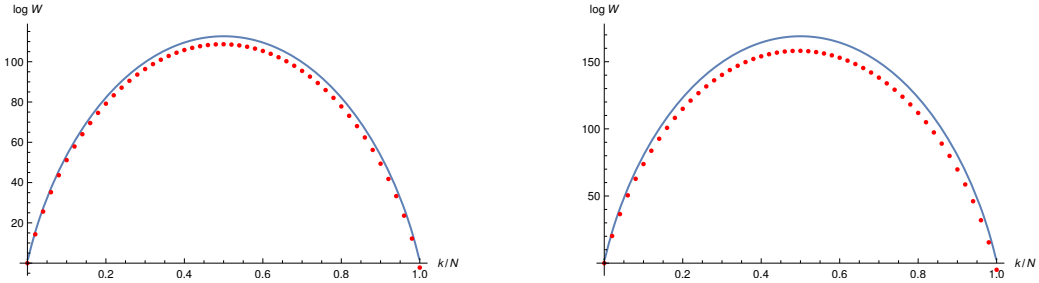

(a) $n = 2$. (b) $n = 3$.

Figure 13. Plot of the $\log W_\lambda$ in the representation $\lambda = [n^k]$ for (a) $n = 2$ and (b) $n = 3$ as a function of k/N with $N = 100$. The red dots are the exact values of $\log W_{[n^k]}$, while the solid curves represent $n \log W_{A_k}$.

6.3 Rectangular Young diagram

In the case of $\mathcal{N} = 4$ SYM, Giant Wilson loops in the representation associated with the rectangular Young diagram are holographically dual to multiple D5 or D3-branes [27, 28]. In the GWW model we also expect that Giant Wilson loops associated with rectangular Young diagram have a simple relation to the (anti-)symmetric Wilson loops. In particular, we expect that the Wilson loop W_λ for the Young diagram $\lambda = [n^k]$ is related to the n-th power of the anti-symmetric Wilson loop $W_{A_k} = W_{[1^k]}$

$$W_{[n^k]} \sim (W_{[1^k]})^n. \tag{6.23}$$

However, we find numerically that the relation (6.23) holds only approximately and in general we have an inequality (see figure 13)

$$\log W_{[n^k]} < n \log W_{[1^k]}. \tag{6.24}$$

The difference $n \log W_{[1^k]} - \log W_{[n^k]}$ might be physically interpreted as the binding energy between multiple Giant loops in GWW model.

JHEP07(2017)030

7 Adjoint model

In this section we consider a unitary matrix model with double trace interaction

$$\mathcal{Z}(N,a)=\int_{\mathrm{U}(N)}dU\exp\Big(a\,\mathrm{Tr}\,U\,\mathrm{Tr}\,U^{\dagger}\Big). \tag{7.1}$$

We call this model the "adjoint model" since $\mathrm{Tr}\,U\,\mathrm{Tr}\,U^{\dagger}=\mathrm{Tr}_{\mathrm{adj}}\,U$ is the trace in the adjoint representation of U(N). This model can be thought of as a truncation of the thermal partition function of free $\mathcal{N}=4$ SYM on $S^3\times S^1$,[7] and it is known that this model exhibits a Hagedorn/deconfinement transition at $a=1$. In the low temperature regime ($a<1$) this model is in the confined phase and the free energy is $\mathcal{O}(N^0)$ while in the high temperature regime ($a>1$) this model is in the deconfined phase and the free energy is $\mathcal{O}(N^2)$.

As discussed in [17], the partition function of the adjoint model $\mathcal{Z}(N,a)$ and that of the GWW model $Z(N,g)$ are related by a certain integral transformation

$$\mathcal{Z}(N,a)=\frac{N^2}{2a}\int_0^{\infty}gdge^{-\frac{N^2g^2}{4a}}Z(N,g). \tag{7.3}$$

Using the exact result of $Z(N,g)$ in (2.4), one can compute $\mathcal{Z}(N,a)$ at finite N by evaluating the integral (7.3) numerically.

Free energy of the adjoint model. Now let us consider the free energy of adjoint model. As emphasized in [17], the partition function of the adjoint model in (7.3) can be naturally written as a sum of two contributions

$$\mathcal{Z}(N,a)=\mathcal{Z}_{\text{th-AdS}}(N,a)+\mathcal{Z}_{\text{BBH}}(N,a), \tag{7.4}$$

where

$$\begin{aligned}\mathcal{Z}_{\text{th-AdS}}(N,a)&=\frac{N^2}{2a}\int_0^{1}gdge^{-\frac{N^2g^2}{4a}}Z(N,g),\\ \mathcal{Z}_{\text{BBH}}(N,a)&=\frac{N^2}{2a}\int_1^{\infty}gdge^{-\frac{N^2g^2}{4a}}Z(N,g),\end{aligned} \tag{7.5}$$

and $\mathcal{Z}_{\text{th-AdS}}(N,a)$ and $\mathcal{Z}_{\text{BBH}}(N,a)$ are interpreted as the contributions of the thermal AdS and the AdS-Schwarzchild black hole (big black hole), respectively. On the bulk gravity side, the deconfinement transition at $a=1$ corresponds to the Hawking-Page transition where the thermal AdS and the big black hole exchange dominance [16].

In the large N limit, the partition function of GWW model $Z(N,g)$ can be replaced by its planer limit $Z(N,g)\approx e^{N^2F_0(g)}$ in (2.7), and it turns out that the g-integral (7.3)

[7] If we turn on the interaction, the thermal partition function can be described by an effective model with one more parameter b [29, 30]

$$\mathcal{Z}(N,a,b)=\int_{\mathrm{U}(N)}dU\exp\left(a|\,\mathrm{Tr}\,U|^2+\frac{b}{N^2}|\,\mathrm{Tr}\,U|^4\right). \tag{7.2}$$

In this paper we only consider the special case $b=0$.

JHEP07(2017)030

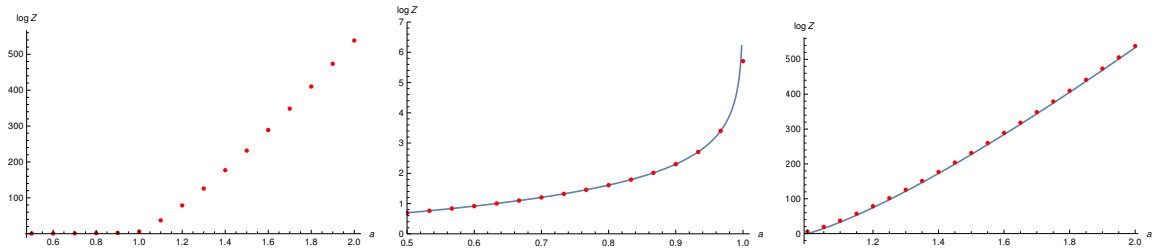

(a) $1/2 < a < 2$. (b) $1/2 < a < 1$. (c) $1 < a < 2$.

Figure 14. Plot of free energy $\log \mathcal{Z}(N, a)$ for $N = 30$ in the range $1/2 < a < 2$. In (a), we show the plot in the whole region $1/2 < a < 2$, while in (b) and (c) we magnify the region $a < 1$ and $a > 1$, respectively. The red dots are the numerical value of the free energy. The solid curves in (b) and (c) represent $-\log(1-a)$ and $N^2\mathcal{F}_0(a)$ in (7.6), respectively.

is dominated by $\mathcal{Z}_{\text{th-AdS}}(N, a)$ in the confined phase ($a < 1$) and by $\mathcal{Z}_{\text{BBH}}(N, a)$ in the deconfined phase ($a > 1$). The free energy of the adjoint model is computed as

$$\log \mathcal{Z}(N, a) \approx \begin{cases} -\log(1-a), & (a < 1), \\ N^2 \mathcal{F}_0(a), & (a > 1), \end{cases} \tag{7.6}$$

where the genus-zero free energy $\mathcal{F}_0(a)$ in the deconfined phase is given by

$$\mathcal{F}_0(a) = -\frac{g_*^2}{4a} + g_* - \frac{1}{2}\log g_* - \frac{3}{4} \tag{7.7}$$

with g_* being the saddle point value of g

$$g_* = a + \sqrt{a(a-1)}. \tag{7.8}$$

As shown in figure 14, the free energy for $N = 30$ evaluated numerically by (7.3) nicely reproduces the analytic result (7.6) at the leading order in the large N expansion. One can proceed to study subleading corrections in the large N expansion. In the deconfined phase $a > 1$, the free energy has a standard genus expansion

$$\log \mathcal{Z}(N, a) = \sum_{\ell=0}^{\infty} N^{2-2\ell} \mathcal{F}_\ell(a). \tag{7.9}$$

In particular, the genus-one free energy is given by

$$\mathcal{F}_1(a) = F_1(g_*) + \log\left[\frac{\sqrt{\pi} N g_*}{a\sqrt{1/a - 1/g_*^2}}\right], \tag{7.10}$$

where $F_1(g)$ is the genus-one free energy of GWW model in (2.10). The second term of (7.10) comes from the Gaussian integral around the saddle point $g = g_*$. As one can see from figure 15, after subtracting the genus-zero part the free energy for $N = 30$ exhibits a nice agreement with the analytic form of one-loop correction (7.10). It would be interesting study the higher genus corrections $\mathcal{F}_\ell(a)$ in (7.9).

JHEP07(2017)030

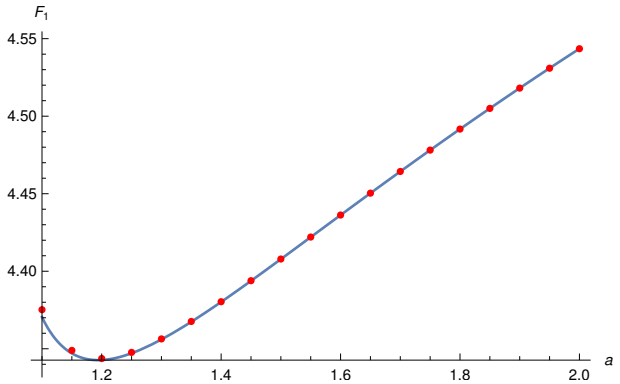

Figure 15. Plot of the genus-one free energy $\mathcal{F}_1(a)$ in the deconfined phase $a > 1$. The red dots are the numerical value of $\log \mathcal{Z}(N, a) - N^2\mathcal{F}_0(a)$ for $N = 30$, while the solid curve is the plot of the analytic form of $\mathcal{F}_1(a)$ in (7.10).

In the confined phase, it is expected that there is a non-perturbative correction to the leading result (7.6) and the apparent singularity at the transition point $a = 1$ is smoothed out [17]. It would be very interesting to study such non-perturbative corrections in detail and find a possible bulk string theory interpretation. We leave this as an interesting future problem.

Winding loops in the adjoint model. The expectation value of Wilson loops in the adjoint model[8] can also be written as a certain integral transform of that of the GWW model. For general operator $\mathcal{O}$, its expectation value $\langle \mathcal{O} \rangle_a$ in the adjoint model is given by[9]

$$\langle \mathcal{O} \rangle_a = \frac{\int dU \mathcal{O} \exp(a \operatorname{Tr} U \operatorname{Tr} U^\dagger)}{\int dU \exp(a \operatorname{Tr} U \operatorname{Tr} U^\dagger)} = \frac{\int_0^\infty dg g e^{-\frac{N^2 g^2}{4a}} \int dU \mathcal{O} \exp[\frac{Ng}{2} \operatorname{Tr}(U + U^\dagger)]}{\int_0^\infty dg g e^{-\frac{N^2 g^2}{4a}} \int dU \exp[\frac{Ng}{2} \operatorname{Tr}(U + U^\dagger)]}. \tag{7.11}$$

In the case of expectation value of winding loops, the integral in the GWW model can be performed in a closed form

$$\langle \operatorname{Tr} U^k \rangle_a = \frac{\int_0^\infty dg g e^{-\frac{N^2 g^2}{4a}} \det(M_0) \operatorname{Tr}(M_0^{-1} M_k)}{\int_0^\infty dg g e^{-\frac{N^2 g^2}{4a}} \det(M_0)}. \tag{7.12}$$

At the leading order in the large N limit, we observed that the integral over g can be replaced by its saddle point value

$$\frac{1}{N} \langle \operatorname{Tr} U^k \rangle_a = \frac{1}{N} \langle \operatorname{Tr} U^k \rangle \Big|_{g=g_*}, \qquad (a > 1, \ N \gg 1) \tag{7.13}$$

In figure 16, we plot the expectation value of winding Wilson loops in the adjoint model. One can see that the leading result (7.13) is reproduced from the numerical evaluation

[8] In the context of $\mathcal{N} = 4$ SYM on $S^3 \times S^1$, Wilson loops in the adjoint model are interpreted as Polyakov loops wrapping the thermal S^1.

[9] This can be thought of as a disorder average over the random coupling g, which is reminiscent of the Sachdev-Ye-Kitaev model [31, 32].

JHEP07(2017)030

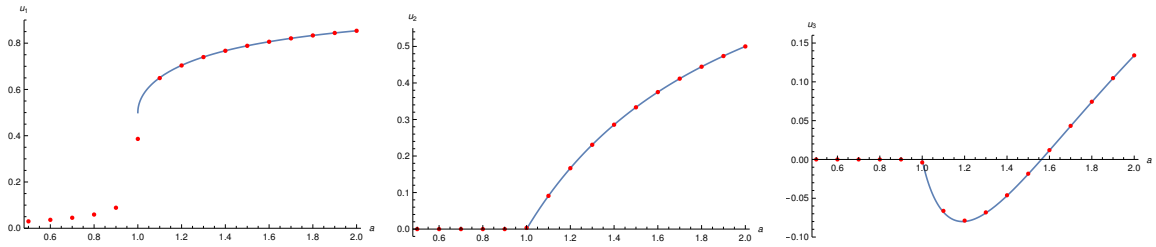

(a) u_1. (b) u_2. (c) u_3.

Figure 16. Plot of the expectation value of the winding Wilson loops $u_k = \frac{1}{N}\langle \mathrm{Tr}\, U^k \rangle_a$ in the adjoint model for $k = 1, 2, 3$. The red dots are the numerical values at $N = 30$, while solid curves represent the large N result in (7.13).

of (7.12) for $N = 30$. As expected, the winding loops are suppressed in the confined phase $a < 1$

$$\lim_{N\to\infty} \frac{1}{N}\langle \mathrm{Tr}\, U^k \rangle_a = 0 \qquad (\forall k \geq 1), \tag{7.14}$$

which is consistent with the absence of non-contractible 1-cycle in the thermal AdS [16]. It would be interesting to study the (non)perturbative correction to the winding loops in the large N expansion.

Giant loops in the adjoint model. Using the integral transformation (7.11), one can compute the expectation value of Wilson loops in the adjoint model in arbitrary representation using the exact result of GWW model

$$\langle \mathrm{Tr}_\lambda\, U \rangle_a = \frac{\int_0^\infty dg g e^{-\frac{N^2 g^2}{4a}} \det\left[I_{\lambda_j+i-j}(Ng)\right]}{\int_0^\infty dg g e^{-\frac{N^2 g^2}{4a}} \det\left[I_{i-j}(Ng)\right]}. \tag{7.15}$$

In particular, we can study Giant Wilson loops of adjoint model in the k-th (anti)symmetric representation in the limit (6.1). At the leading order in the large N limit, the g-integral is approximated by the saddle point value $g = g_*$. We have checked numerically that the result of [12] is reproduced. As we can see from figure 17, the expectation values of Giant loops are suppressed in the confined phase $a < 1$. In the deconfined phase, Giant loop in the symmetric representation W_{S_k} is exponentially suppressed when $x = k/N$ becomes larger than some critical value x_{cr}, as observed in [12]. It is argued that this is consistent with the absence of D3-brane solution corresponding to W_{S_k} in the black hole background [12, 26]. It would be interesting to study the critical value x_{cr} as a function of a and see if it has some physical interpretation on the dual black hole side.

8 Discussion

In this paper we have studied the free energy and Wilson loops in the GWW model and the adjoint model using the exact result at finite N. For the GWW model the exact finite N result correctly reproduces the known large N expansion of free energy and Wilson loops. We have also seen that one can extract the (non)perturbative corrections in the large N

JHEP07(2017)030

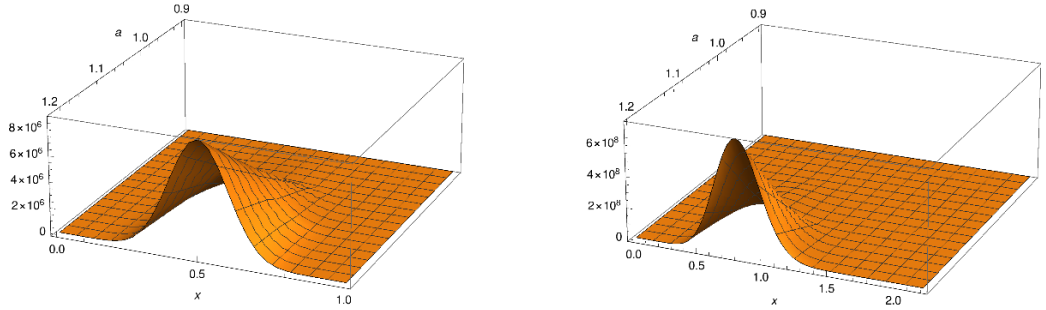

(a) Anti-symmetric representation W_{A_k}.

(b) Symmetric representation W_{S_k}.

Figure 17. Plot of the expectation value of Wilson loops in (a) the anti-symmetric representation and (b) the symmetric representation, as functions of a and $x = k/N$ for $N = 30$.

expansion from the exact finite N result by numerical fitting, and some of the results in this paper are new. It would be interesting to develop an analytic method to compute such (non)perturbative corrections and see if our numerical results are reproduced from analytic computation.

We have seen that the large N expansion of free energy and Wilson loops behaves quite differently between the gapped phase and the ungapped phase of GWW model. In the gapped phase the genus expansion is Borel non-summable and the perturbative and non-perturbative corrections are related by resurgence [9]. On the other hand, in the ungapped phase, the perturbative corrections stop at first order. Although the instanton coefficient in the ungapped phase has an all order expansion in $1/N$, this series is Borel summable and the each instanton sector seems to be closed by itself (see appendix C for details). This is in stark contrast to the situation in the gapped phase and it would be interesting to see how these two expansions are connected as we cross the transition point $g = 1$.

We proposed a master field of GWW model from the exact result of characteristic polynomial at finite N. We found that this master field has an interesting eigenvalue distribution. In the gapped phase the eigenvalue distribution approaches the known gapped distribution on the unit circle as N becomes large. On the other hand, in the ungapped phase we observed that the eigenvalues are distributed inside the unit circle and we find numerically that the eigenvalues are located along the contour $\Phi(z) = -S_{\text{inst}}(g)$ of constant effective potential. We do not have a proof of the last statement and it would be interesting to show this analytically. Also, it is not clear whether the distribution on the contour $\Phi(z) = -S_{\text{inst}}(g)$ satisfies the saddle point equation of GWW model or not. It would be very interesting to clarify the physical interpretation, if any, of this distribution further.

We have also studied Giant Wilson loops in both the GWW model and the adjoint model. In particular, in the adjoint model Giant Wilson loops are expected to be holographically dual to some configuration of D-branes. We hope that our finite N analysis will shed light on the behavior of D-branes in black hole background or the black hole itself beyond the supergravity approximation.

JHEP07(2017)030

Acknowledgments

I would like to thank Pavel Buividovich, Gerald Dunne, Marcos Marino, Shunya Mizoguchi, Takeshi Morita, Tomoki Nosaka, Semen Valgushev, and Yasuhiko Yamada for useful discussions and correspondences. This work was supported in part by JSPS KAKENHI Grant Number 16K05316.

A Exact result of GWW model

In this appendix we review the exact result of partition function and Wilson loops in GWW model at finite N.

Let us first consider the following integral with some function f

$$I^f = \int_{\mathrm{U}(N)} dU \det\left[f(U)\right] e^{\frac{Ng}{2}\mathrm{Tr}(U+U^\dagger)}. \tag{A.1}$$

This can be rewritten as an integral over the eigenvalues $\{e^{\mathrm{i}\theta_j}\}_{j=1,\cdots,N}$ of unitary matrix U

$$I^f = \frac{1}{N!}\int_0^{2\pi} |\Delta|^2 \prod_{j=1}^N \frac{d\theta_j}{2\pi} e^{Ng\cos\theta_j} f(e^{\mathrm{i}\theta_j}), \tag{A.2}$$

where Δ denotes the Vandermonde determinant

$$\Delta = \sum_{\sigma\in S_N} (-1)^\sigma \prod_{j=1}^N e^{\mathrm{i}(N-j)\theta_{\sigma(j)}}. \tag{A.3}$$

Plugging (A.3) into (A.2), we get a double sum over S_N. Since the integrand is symmetric under the permutation of variables θ_j, one can show that this sum can be reduced to a single sum over S_N

$$I^f = \sum_{\sigma\in S_N} (-1)^\sigma \prod_{j=1}^N \int_0^{2\pi} \frac{d\theta_j}{2\pi} e^{\mathrm{i}(\sigma(j)-j)\theta_j} e^{Ng\cos\theta_j} f(e^{\mathrm{i}\theta_j}) = \det\left[I^f_{i-j}\right]_{i,j=1,\cdots,N}, \tag{A.4}$$

where we defined

$$I^f_m = \int_0^{2\pi} \frac{d\theta}{2\pi} e^{\mathrm{i}m\theta} e^{Ng\cos\theta} f(e^{\mathrm{i}\theta}). \tag{A.5}$$

For the computation of partition function, we set $f = 1$. Then the integral (A.5) is nothing but the modified Bessel function of the first kind $I_m(Ng)$, and we recover the exact result of partition function at finite N in (2.4).

For the computation of winding Wilson loop $\mathrm{Tr}\, U^k$, we set

$$f(U) = 1 + tU^k \tag{A.6}$$

and pick up the linear term of t in the small t expansion

$$\det\left[f(U)\right] = 1 + t\,\mathrm{Tr}\, U^k + \mathcal{O}(t^2). \tag{A.7}$$

JHEP07(2017)030

For this choice of f, the integral I_m^f in (A.5) becomes

$$I_m^f = I_m(Ng) + tI_{k+m}(Ng), \tag{A.8}$$

and we find

$$I^f = \det\Big[I_{i-j}(Ng) + tI_{k+i-j}(Ng)\Big] = \det(M_0 + tM_k). \tag{A.9}$$

Here the $N \times N$ matrix M_k has been defined in (3.2). Picking up the linear term in t and normalizing by the partition function $Z(N,g) = \det M_0$, we find that the expectation value of winding Wilson loop $\langle \mathrm{Tr}\, U^k \rangle$ is given by (3.1). In a similar manner, one can show the relation (4.2)

$$\begin{aligned}\langle \det(x-U)\rangle &= \frac{1}{Z(N,g)}\int dU \det(x-U) e^{\frac{Ng}{2}\mathrm{Tr}(U+U^\dagger)} \\ &= \frac{\det(xM_0 - M_1)}{\det M_0} = \det(x - M_0^{-1}M_1).\end{aligned} \tag{A.10}$$

Lastly, let us consider the expectation value of the character $\mathrm{Tr}_\lambda U = \chi_\lambda(U)$ of $\mathrm{U}(N)$ group

$$\chi_\lambda(U) = \frac{1}{\Delta}\sum_{\sigma\in S_N}(-1)^\sigma \prod_{j=1}^N e^{\mathrm{i}(\lambda_j + N - j)\theta_{\sigma(j)}}. \tag{A.11}$$

Again, the factor $|\Delta|^2\chi_\lambda(U)$ becomes a double sum over the permutation group S_N, but this sum can be reduced to a single sum upon integration and we find

$$\int dU \chi_\lambda(U) e^{\frac{Ng}{2}\mathrm{Tr}(U+U^\dagger)} = \sum_{\sigma\in S_N}(-1)^\sigma \prod_{j=1}^N \int_0^{2\pi}\frac{d\theta_j}{2\pi} e^{\mathrm{i}(\lambda_j - j + \sigma(j))\theta_j} e^{Ng\cos\theta_j} = \det\Big[I_{\lambda_j+i-j}(Ng)\Big]. \tag{A.12}$$

After dividing by the partition function, we recover the result of $\langle \mathrm{Tr}_\lambda U\rangle$ in (5.1).

B Effective potential in the ungapped phase

In this appendix, we explain the computation of the effective potential $\Phi(z)$ in (4.6) following the argument in [11]. As discussed in [11], the eigenvalue integral (A.2) can be rewritten as a holomorphic integral with complex variable $z_j = e^{\mathrm{i}\theta_j}$. For the partition function we find

$$Z(N,g) = \frac{1}{N!}\int \prod_{j=1}^N \frac{dz_j}{2\pi\mathrm{i}} e^{-NW(z_j)} \prod_{i<j}(z_i - z_j)^2, \tag{B.1}$$

where the potential $W(z)$ is given by

$$W(z) = -\frac{g}{2}(z + z^{-1}) + \log z. \tag{B.2}$$

The integral (B.1) has the same form as the hermitian matrix model, although the integral contour is different: in the unitary matrix model the integral contour is along the unit circle $|z_j| = 1$ while in the hermitian matrix model the integral is along the real axis $z_j \in \mathbb{R}$. At

JHEP07(2017)030

least formally, the saddle point equation for the eigenvalue integral (B.1) takes the same form as that of the hermitian matrix model

$$W'(z_i) - \frac{2}{N}\sum_{j\neq i}\frac{1}{z_i - z_j} = 0. \tag{B.3}$$

Then one can show that the resolvent defined by

$$\omega(z) = \frac{1}{N}\sum_{i=1}^{N}\frac{1}{z - z_i} \tag{B.4}$$

satisfies the loop equation

$$\omega(z)^2 + \frac{1}{N}\omega'(z) - W'(z)\omega(z) + f(z) = 0, \tag{B.5}$$

where $f(z)$ is given by

$$f(z) = \frac{1}{N}\sum_{i=1}^{N}\frac{W'(z) - W'(z_i)}{z - z_i}. \tag{B.6}$$

In the planar limit, the second term of (B.5) can be omitted and the loop equation can be written as an algebraic equation defining a spectral curve

$$y^2 = W'(z)^2 - 4f(z) \tag{B.7}$$

with y being

$$y = W'(z) - 2\omega(z). \tag{B.8}$$

As emphasized in [33], the quantity y has an elegant physical interpretation as the force acting on an eigenvalue if it tries to move away from its stationary position. This suggests that it is natural to define an effective potential as the integral of force: $U(z) = \int^z y dz$. However, as discussed in [11], it is more appropriate to take the real part of $\int^z y dz$ and define the effective potential as

$$\Phi(z) = \mathrm{Re}\int^z y dz, \tag{B.9}$$

since the dominance to the eigenvalue integral (B.1) is dictated by the real part of potential. One can show that the potential $\Phi(z)$ is constant on each cut made by the condensation of eigenvalues in the large N limit.

Now let us compute the effective potential in the ungapped phase of GWW model. To do this, we notice that the planar resolvent in the gapped phase has a simple expansion in the large z region

$$\omega(z) = \frac{1}{z} + \sum_{k=1}^{\infty}\frac{1}{N}\langle \mathrm{Tr}\, U^k\rangle\frac{1}{z^{k+1}} = \frac{1}{z} + \frac{g}{2z^2}, \tag{B.10}$$

since winding Wilson loops $\langle \mathrm{Tr}\, U^k\rangle$ vanish except for $k = 1$ (see (3.4) and (3.5)). Then the quantity y in (B.8) is given by

$$y = -\frac{g}{2}\left(1 + \frac{1}{z^2}\right) - \frac{1}{z}, \tag{B.11}$$

JHEP07(2017)030

and the spectral curve (B.7) becomes

$$y^2 = \left[\frac{g}{2}\left(1+\frac{1}{z^2}\right)+\frac{1}{z}\right]^2. \tag{B.12}$$

This curve has two branches and we should be careful about the sign of y. Assuming that the eigenvalues are distributed along the unit circle $|z|=1$, the sign of y should change as we cross the line $|z|=1$

$$y = \begin{cases} -\dfrac{g}{2}\left(1+\dfrac{1}{z^2}\right)-\dfrac{1}{z}, & (|z|>1), \\ +\dfrac{g}{2}\left(1+\dfrac{1}{z^2}\right)+\dfrac{1}{z}, & (|z|<1), \end{cases} \tag{B.13}$$

One can show that the eigenvalue density $\rho(\theta)$ (2.8) is reproduced from the discontinuity along $|z|=1$. Finally, the effective potential $\Phi(z)$ is given by the integral (B.9) and we arrive at the result (4.6).

C Instanton correction in the ungapped phase

In this appendix, we consider the instanton correction of free energy in the ungapped phase of GWW model. Here (and only in this appendix) we use the convention of string coupling g_s and 't Hooft coupling t in footnote 1:

$$Z(N,g_s) = \int_{\mathrm{U}(N)} dU \exp\left[\frac{1}{2g_s}\mathrm{Tr}(U+U^\dagger)\right] = \det\left[I_{i-j}(1/g_s)\right]_{i,j=1,\cdots,N}. \tag{C.1}$$

We are interested in the instanton corrections in the 't Hooft limit

$$N\to\infty, \quad g_s\to 0, \qquad t = Ng_s: \text{ fixed}. \tag{C.2}$$

Instanton corrections to the free energy in the gapped phase $t<1$ have been studied extensively in [9]. Here we would like to point out that the first non-zero instanton correction to the free energy in the ungapped phase $t>1$ can be written in a closed form.

To study the (non)perturbative corrections to the free energy, it is convenient to use the method of orthogonal polynomial $p_n(z)$ obeying

$$\oint \frac{dz}{2\pi \mathrm{i} z} e^{\frac{1}{2g_s}(z+z^{-1})} p_n(z) p_m(z^{-1}) = h_n \delta_{n,m}. \tag{C.3}$$

The partition function of GWW model is written in terms of the norm h_n as

$$Z(N,g_s) = \prod_{n=0}^{N-1} h_n. \tag{C.4}$$

From the constant term f_n of $p_n(z)$[10]

$$f_n = (-1)^n p_n(0) \tag{C.5}$$

[10]Note that we have shifted the index n of f_n by one as compared to the definition of [9].

JHEP07(2017)030

we can compute the ratio of the norm h_n

$$\frac{h_n}{h_{n-1}} = 1 - f_n^2. \tag{C.6}$$

From (C.4) and (C.6) one can show that

$$\frac{Z(N+1, g_s)Z(N-1, g_s)}{Z(N, g_s)^2} = 1 - f_N^2. \tag{C.7}$$

Furthermore, using the recursion relation

$$p_n(z) = zp_{n-1}(z) + (-1)^n f_n z^{n-1} p_{n-1}(z^{-1}), \tag{C.8}$$

one can show that f_n satisfies

$$2g_s n f_n = (1 - f_n^2)(f_{n+1} + f_{n-1}). \tag{C.9}$$

Note that this is known as a discrete Painlevé equation [34, 35]. From Heine's formula the orthogonal polynomial $p_n(z)$ with $n = N$ is simply given by the expectation value of the characteristic polynomial in the U(N) GWW model

$$p_N(z) = \langle \det(z - U) \rangle. \tag{C.10}$$

This also implies that f_n (C.5) with $n = N$ is given by the expectation value of $\det U$

$$f_N = \langle \det U \rangle = \frac{\det\left[I_{1+i-j}(1/g_s)\right]}{\det\left[I_{i-j}(1/g_s)\right]}. \tag{C.11}$$

In the 't Hooft limit (C.2), f_N becomes a function $f(t, g_s)$ of the 't Hooft coupling t and the string coupling g_s. Then $f(t, g_s)$ satisfies the continuum version of the recursion relation (C.9)

$$2tf(t, g_s) = \Big(1 - f(t, g_s)^2\Big)\Big(f(t + g_s, g_s) + f(t - g_s, g_s)\Big). \tag{C.12}$$

This is called the *pre-string* equation. Once we know the function $f(t, g_s)$, we can compute the free energy $F(t, g_s)$ from the continuum limit of (C.7)

$$F(t, g_s) = \frac{1}{4\sinh^2 \frac{g_s \partial_t}{2}} \log R(t, g_s), \tag{C.13}$$

where $R(t, g_s)$ is defined by

$$R(t, g_s) = 1 - f(t, g_s)^2. \tag{C.14}$$

In the ungapped phase, $f(t, g_s)$ is exponentially small. Thus the relation (C.12) is approximated by

$$2tf^{(1)}(t, g_s) = f^{(1)}(t + g_s, g_s) + f^{(1)}(t - g_s, g_s), \tag{C.15}$$

JHEP07(2017)030

where we have introduced the notation $f^{(1)}(t, g_s)$ for the one-instanton correction to $f(t, g_s)$. We notice that this is exactly the recursion relation of Bessel function $J_\nu(x)$

$$2Ng_s J_N(1/g_s) = J_{N+1}(1/g_s) + J_{N-1}(1/g_s). \tag{C.16}$$

Thus we expect that $f(t, g_s)$ is proportional to $J_N(1/g_s) = J_N(N/t)$, which is consistent with the large N behavior of $\langle \det U \rangle$ studied in [22].

As discussed in [9], we can fix the proportionality constant by comparing the double-scaling limit of $J_N(N/t)$ and the Hastings-McLeod solution of the Painlevé II equation. In the double scaling limit

$$f = g_s^{1/3} u, \quad t = 1 - g_s^{2/3}\kappa, \quad g_s \to 0, \tag{C.17}$$

$u(\kappa)$ satisfies the Painlevé II equation

$$u'' - 2u^3 + 2\kappa u = 0. \tag{C.18}$$

There is a unique real solution (Hastings-McLeod solution) for $\kappa \in \mathbb{R}$ with the asymptotic behavior

$$u = \begin{cases} \sqrt{\kappa}, & (\kappa \to \infty), \\ 2^{\frac{1}{3}} \mathrm{Ai}(-2^{\frac{1}{3}}\kappa), & (\kappa \to -\infty). \end{cases} \tag{C.19}$$

One can compare this with the double scaling limit of the Bessel function [36]

$$\lim_{N\to\infty} N^{\frac{1}{3}} J_N(N + N^{\frac{1}{3}}\kappa) = 2^{\frac{1}{3}} \mathrm{Ai}(-2^{\frac{1}{3}}\kappa). \tag{C.20}$$

From (C.19) and (C.20), we conclude that the proportionality constant is 1

$$f^{(1)}(t, g_s) = J_N(N/t), \qquad N = \frac{t}{g_s}. \tag{C.21}$$

Now we can study the genus expansion of 1-instanton coefficients in the ungapped phase ($t > 1$) using the so-called Debye expansion of Bessel function [37]

$$J_N(N/\cosh\alpha) = \frac{e^{-N(\alpha - \tanh\alpha)}}{\sqrt{2\pi N \tanh\alpha}} \sum_{k=0}^{\infty} \frac{U_k(\coth\alpha)}{N^k}, \tag{C.22}$$

where $U_k(x)$ is a polynomial defined recursively from $U_0 = 1$

$$U_{k+1}(x) = \frac{1}{2}x^2(1-x^2)U_k'(x) + \frac{1}{8}\int_0^x dy(1-5y^2)U_k(y). \tag{C.23}$$

The first three terms are given by

$$\begin{aligned} U_1(x) &= \frac{-5x^3 + 3x}{24}, \\ U_2(x) &= \frac{385x^6 - 462x^4 + 81x^2}{1152}, \\ U_3(x) &= \frac{-425425x^9 + 765765x^7 - 369603x^5 + 30375x^3}{414720}. \end{aligned} \tag{C.24}$$

JHEP07(2017)030

From (C.21) and (C.22), we identify $\cosh\alpha = t$. Finally we arrive at a closed form of 1-instanton correction in the ungapped phase

$$f^{(1)}(t,g_s) = \sqrt{\frac{g_s}{2\pi}}\frac{e^{-\frac{1}{g_s}A(t)}}{(t^2-1)^{1/4}}\sum_{k=0}^{\infty} g_s^k t^{-k} U_k\left(\frac{t}{\sqrt{t^2-1}}\right), \tag{C.25}$$

where the instanton action $A(t)$ is given by

$$A(t) = t(\alpha - \tanh\alpha) = t\cosh^{-1}(t) - \sqrt{t^2-1}. \tag{C.26}$$

From the relation (C.14) the two-instanton correction to $R(t,g_s)$ is given by

$$\begin{aligned} R^{(2)}(t,g_s) &= -f^{(1)}(t,g_s)^2 \\ &= -\frac{g_s}{2\pi}\frac{e^{-\frac{2}{g_s}A(t)}}{\sqrt{t^2-1}}\left[\sum_{k=0}^{\infty} g_s^k t^{-k} U_k\left(\frac{t}{\sqrt{t^2-1}}\right)\right]^2 \\ &= -\frac{g_s}{2\pi}\frac{e^{-\frac{2}{g_s}A(t)}}{\sqrt{t^2-1}}\left[1 - g_s\frac{2t^2+3}{12\,(t^2-1)^{3/2}} + g_s^2\frac{4t^4+156t^2+45}{288\,(t^2-1)^3} + \cdots\right]. \end{aligned} \tag{C.27}$$

This agrees with the result of [9] obtained by solving the *pre-string* equation (C.12), but the overall factor was not determined in [9]. We have fixed the overall normalization of $R^{(2)}(t,g_s)$ as discussed above. Now the result (C.27) can be easily translated to the two-instanton correction to the free energy using the relation (C.13)

$$F^{(2\text{-inst})} = -\frac{\widehat{g}_s}{8\pi}e^{-\frac{2}{g_s}A(t)}\left[1 - \widehat{g}_s\frac{26t^2+9}{12} + \widehat{g}_s^2\frac{964t^4+2484t^2+297}{288} + \cdots\right], \tag{C.28}$$

where we have introduced the rescaled coupling $\widehat{g}_s$ by

$$\widehat{g}_s = \frac{g_s}{(t^2-1)^{3/2}}. \tag{C.29}$$

It is interesting to consider the Borel summability of the Debye expansion in (C.25). Let us consider the Borel sum

$$\mathcal{B}\left[\sum_{k=0}^{\infty} g_s^k t^{-k} U_k\left(\frac{t}{\sqrt{t^2-1}}\right)\right] = \int_0^{\infty}\frac{d\zeta}{g_s}e^{-\frac{\zeta}{g_s}}\sum_{k=0}^{\infty}\frac{\zeta^k}{k!}t^{-k}U_k\left(\frac{t}{\sqrt{t^2-1}}\right). \tag{C.30}$$

As we can see from figure 18, there is no pole on the positive real axis on the Borel plane and hence the expansion of $f^{(1)}(t,g_s)$ in (C.25) is Borel summable. We have checked numerically that the Borel resummation of $f^{(1)}(t,g_s)$ agrees with the original expression of Bessel function (C.21). This is in a stark contrast to the situation in the gapped phase. As shown in [9], in the gapped phase the genus expansion of free energy is Borel non-summable and the perturbative part and the non-perturbative part are related by the resurgence. On the other hand, in the ungapped phase the perturbative genus expansion of free energy is not an infinite power series but stops at genus-zero. Although the one-instanton coefficient has infinite series expansion in g_s, it is Borel summable as we have seen above.

JHEP07(2017)030

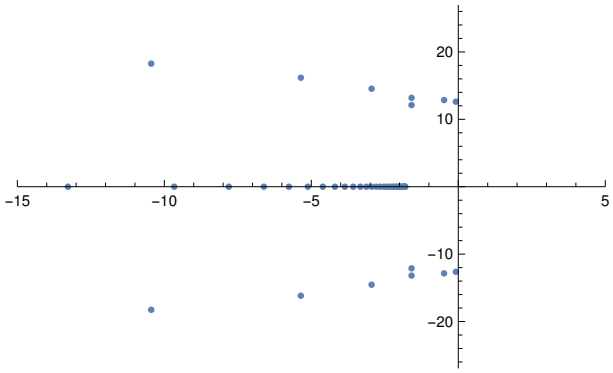

Figure 18. Poles of the integrand of (C.30) on the Borel ζ-plane for $t = 2$.

D Resolvent of GWW model

In this appendix we consider the genus-one resolvent of GWW model in the gapped phase, from which we can extract the genus-one correction to the winding Wilson loops and compare with the result of numerical fitting (3.6). To do this, we use the relation between unitary matrix model and hermitian matrix model [23] and the formula of genus-one resolvent of hermitian matrix model [38].

As shown in [23], a unitary matrix model can be written as a hermitian matrix model

$$\int dU e^{-N \operatorname{Tr} V(U)} = \int dM e^{-N \operatorname{Tr} W(M)} \tag{D.1}$$

where the eigenvalue t of unitary matrix U and the eigenvalue z of hermitian matrix M are related by

$$t = \frac{1 + \mathrm{i}z}{1 - \mathrm{i}z}, \tag{D.2}$$

and the potentials in (D.1) are related by

$$W(z) = V(t) + \log(1 + z^2). \tag{D.3}$$

In the case of GWW model the potential are given by

$$V(t) = -\frac{g}{2}(t + t^{-1}), \qquad W(z) = g\frac{z^2 - 1}{z^2 + 1} + \log(1 + z^2). \tag{D.4}$$

We define the resolvent $\omega(z)$ of hermitian matrix model and the resolvent $v(t)$ of unitary matrix model as

$$\begin{aligned} \omega(z) &= \frac{1}{N}\left\langle \operatorname{Tr} \frac{1}{z - M} \right\rangle, \\ v(t) &= \frac{\mathrm{i}}{N}\left\langle \operatorname{Tr} \frac{t + U}{t - U} \right\rangle, \end{aligned} \tag{D.5}$$

and they are related by

$$v(t) = (1 + z^2)\omega(z) - z. \tag{D.6}$$

In the large N limit these resolvents have genus expansion

$$\omega(z) = \sum_{\ell=0}^{\infty} N^{-2\ell}\omega_\ell(z), \qquad v(t) = \sum_{\ell=0}^{\infty} N^{-2\ell} v_\ell(t). \tag{D.7}$$

Using the technique developed in [38] for hermitian matrix model, one can compute the higher genus correction of resolvent $\omega_\ell(z)$ recursively. In what follows we assume that the hermitian matrix model is in the one-cut phase, i.e. eigenvalues are distributed along the cut $z \in [-A, A]$ on the real axis.

Genus-zero resolvent. Let us first consider the genus-zero resolvent which is given by the general formula

$$\omega_0(z) = \int_C \frac{dx}{4\pi \mathrm{i}} \frac{W'(x)}{z-x} \sqrt{\frac{z^2-A^2}{x^2-A^2}}, \tag{D.8}$$

where the contour C encircles the cut $[-A, A]$. From the condition

$$\lim_{z\to\infty} \omega_0(z) = \frac{1}{z} + \mathcal{O}(z^{-2}) \tag{D.9}$$

we find

$$\int_C \frac{dx}{4\pi \mathrm{i}} \frac{W'(x)}{\sqrt{x^2-A^2}} = 0, \qquad \int_C \frac{dx}{4\pi \mathrm{i}} \frac{xW'(x)}{\sqrt{x^2-A^2}} = 1. \tag{D.10}$$

From these conditions we can fix the end-point of cut A as a function of coupling g

$$A = \frac{1}{\sqrt{g-1}}. \tag{D.11}$$

Picking up the residue of poles at $x = \pm \mathrm{i}$ and $x = \infty$ in (D.8), the genus-zero resolvent becomes

$$\omega_0(z) = \frac{1}{2}\left[W'(z) - M(z)\sqrt{z^2-A^2}\right], \qquad M(z) = \frac{4\sqrt{1+A^2}}{A^2(1+z^2)^2}. \tag{D.12}$$

Then using the dictionary between resolvents of hermitian and unitary matrix models (D.6), we arrive at the genus-zero resolvent of GWW model

$$v_0(t) = \frac{2g}{1+z^2}\left[z - \sqrt{z^2 - g^{-1}(1+z^2)}\right]. \tag{D.13}$$

We note in passing that one can easily show that this agrees with the integral over the eigenvalues $e^{\mathrm{i}\theta}$ with the weight $\rho(\theta)$ in the gapped phase (2.8)

$$\frac{\mathrm{i}}{2} v_0(t) = \frac{1}{2}\int d\theta \rho(\theta) \frac{1+te^{\mathrm{i}\theta}}{1-te^{\mathrm{i}\theta}} = \frac{g(t+1)}{4t}\left[t - 1 + \sqrt{(t-1)^2 + \frac{4t}{g}}\right]. \tag{D.14}$$

Genus-one resolvent. Let us move on to the genus-one resolvent. The genus-one resolvent in the one-cut phase of hermitian matrix model is given by [38]

$$\omega_1(z) = \frac{\chi_+^{(2)} + \chi_-^{(2)}}{16} - \frac{\chi_+^{(1)} - \chi_-^{(1)}}{16A}, \tag{D.15}$$

JHEP07(2017)030

where $\chi_{\pm}^{(1)}$ and $\chi_{\pm}^{(2)}$ are defined by

$$\begin{aligned}\chi_{\pm}^{(1)} &= \frac{1}{M_1\sqrt{z^2-A^2}(z\mp A)},\\ \chi_{\pm}^{(2)} &= \frac{1}{M_1\sqrt{z^2-A^2}(z\mp A)^2}\mp\frac{M_2\chi_{\pm}^{(1)}}{M_1},\end{aligned} \tag{D.16}$$

and the moment M_k is defined by

$$M_k=\int_C\frac{dx}{2\pi\mathrm{i}}\frac{W'(x)}{(x-A)^k\sqrt{x^2-A^2}}=\frac{1}{(k-1)!}\frac{d^{k-1}}{dz^{k-1}}M(z)\Big|_{z=A}. \tag{D.17}$$

From the explicit form of function $M(z)$ in (D.12), the moments are evaluated as

$$M_1=\frac{4}{A^2(1+A^2)^{\frac{3}{2}}},\qquad M_2=-\frac{16}{A(1+A^2)^{\frac{5}{2}}}. \tag{D.18}$$

Plugging (D.16) and (D.18) into (D.15), we find the closed form of genus-one resolvent

$$\omega_1(z)=\frac{A^4\sqrt{1+A^2}(2z^2+1-A^2)}{16(z^2-A^2)^{\frac{5}{2}}}. \tag{D.19}$$

We can translated this result to the unitary GWW model using the dictionary (D.6)

$$\begin{aligned}\frac{\mathrm{i}}{2}v_1(t)&=\frac{\mathrm{i}}{2}(1+z^2)\omega_1(z)\\ &=\frac{t(t+1)}{8(g-1)g^2}\left[-g\left((t-1)^2+\frac{4t}{g}\right)^{-\frac{3}{2}}+4t(g-1)\left((t-1)^2+\frac{4t}{g}\right)^{-\frac{5}{2}}\right].\end{aligned} \tag{D.20}$$

Finally, we can see that the small t expansion of $v_1(t)$ reproduces the genus-one part of winding Wilson loops in (3.6)

$$\begin{aligned}\frac{\mathrm{i}}{2}v_1(t)=&-\frac{t}{8(g-1)g}+\frac{t^2}{4(g-1)g^2}+\frac{(10-28g+15g^2)t^3}{8(g-1)g^3}\\ &+\frac{(-35+90g-70g^2+16g^3)t^4}{2(g-1)g^4}+\frac{5\left(35g^4-260g^3+630g^2-616g+210\right)t^5}{8(g-1)g^5}\\ &+\frac{\left(192g^5-2135g^4+8120g^3-13860g^2+10920g-3234\right)t^6}{4(g-1)g^6}+\cdots.\end{aligned} \tag{D.21}$$

References

[1] Y. Hatsuda, S. Moriyama and K. Okuyama, *Exact results on the ABJM Fermi gas*, *JHEP* **10** (2012) 020 [arXiv:1207.4283] [INSPIRE].

JHEP07(2017)030

[2] Y. Hatsuda, S. Moriyama and K. Okuyama, *Instanton effects in ABJM theory from Fermi gas approach*, *JHEP* **01** (2013) 158 [arXiv:1211.1251] [INSPIRE].

[3] Y. Hatsuda, S. Moriyama and K. Okuyama, *Instanton bound states in ABJM theory*, *JHEP* **05** (2013) 054 [arXiv:1301.5184] [INSPIRE].

[4] Y. Hatsuda, M. Mariño, S. Moriyama and K. Okuyama, *Non-perturbative effects and the refined topological string*, *JHEP* **09** (2014) 168 [arXiv:1306.1734] [INSPIRE].

[5] D.J. Gross and E. Witten, *Possible third order phase transition in the large N lattice gauge theory*, *Phys. Rev.* **D 21** (1980) 446 [INSPIRE].

[6] S.R. Wadia, *A study of* U(N) *lattice gauge theory in* 2*-dimensions*, preprint EFI-79/44, University of Chicago, Chicago IL U.S.A., (1979) [arXiv:1212.2906] [INSPIRE].

[7] V. Periwal and D. Shevitz, *Unitary matrix models as exactly solvable string theories*, *Phys. Rev. Lett.* **64** (1990) 1326 [INSPIRE].

[8] I.R. Klebanov, J.M. Maldacena and N. Seiberg, *Unitary and complex matrix models as* 1D *type* 0 *strings*, *Commun. Math. Phys.* **252** (2004) 275 [hep-th/0309168] [INSPIRE].

[9] M. Mariño, *Nonperturbative effects and nonperturbative definitions in matrix models and topological strings*, *JHEP* **12** (2008) 114 [arXiv:0805.3033] [INSPIRE].

[10] P.V. Buividovich, G.V. Dunne and S.N. Valgushev, *Complex path integrals and saddles in two-dimensional gauge theory*, *Phys. Rev. Lett.* **116** (2016) 132001 [arXiv:1512.09021] [INSPIRE].

[11] G. Álvarez, L. Martínez Alonso and E. Medina, *Complex saddles in the Gross-Witten-Wadia matrix model*, *Phys. Rev.* **D 94** (2016) 105010 [arXiv:1610.09948] [INSPIRE].

[12] G. Grignani, J.L. Karczmarek and G.W. Semenoff, *Hot giant loop holography*, *Phys. Rev.* **D 82** (2010) 027901 [arXiv:0904.3750] [INSPIRE].

[13] J.L. Karczmarek, G.W. Semenoff and S. Yang, *Comments on k-strings at large-N*, *JHEP* **03** (2011) 075 [arXiv:1012.5875] [INSPIRE].

[14] J.L. Karczmarek and G.W. Semenoff, *Large representation recurrences in large-N random unitary matrix models*, *JHEP* **10** (2011) 066 [arXiv:1108.2712] [INSPIRE].

[15] B. Sundborg, *The Hagedorn transition, deconfinement and* $N = 4$ *SYM theory*, *Nucl. Phys.* **B 573** (2000) 349 [hep-th/9908001] [INSPIRE].

[16] E. Witten, *Anti-de Sitter space, thermal phase transition and confinement in gauge theories*, *Adv. Theor. Math. Phys.* **2** (1998) 505 [hep-th/9803131] [INSPIRE].

[17] H. Liu, *Fine structure of Hagedorn transitions*, hep-th/0408001 [INSPIRE].

[18] I. Bars and F. Green, *Complete integration of* U(N) *lattice gauge theory in a large N limit*, *Phys. Rev.* **D 20** (1979) 3311 [INSPIRE].

[19] P. Rossi, M. Campostrini and E. Vicari, *The large-N expansion of unitary matrix models*, *Phys. Rept.* **302** (1998) 143 [hep-lat/9609003] [INSPIRE].

[20] Y.Y. Goldschmidt, 1/N *expansion in two-dimensional lattice gauge theory*, *J. Math. Phys.* **21** (1980) 1842 [INSPIRE].

[21] F. Green and S. Samuel, *Calculating the large-N phase transition in gauge and matrix models*, *Nucl. Phys.* **B 194** (1982) 107 [INSPIRE].

JHEP07(2017)030

[22] P. Rossi, *On the exact evaluation of* $\langle \det U_p \rangle$ *in a lattice gauge model*, *Phys. Lett.* **B 117** (1982) 72 [INSPIRE].

[23] S. Mizoguchi, *On unitary/Hermitian duality in matrix models*, *Nucl. Phys.* **B 716** (2005) 462 [hep-th/0411049] [INSPIRE].

[24] N. Drukker and B. Fiol, *All-genus calculation of Wilson loops using D-branes*, *JHEP* **02** (2005) 010 [hep-th/0501109] [INSPIRE].

[25] S. Yamaguchi, *Wilson loops of anti-symmetric representation and D5-branes*, *JHEP* **05** (2006) 037 [hep-th/0603208] [INSPIRE].

[26] S.A. Hartnoll and S.P. Kumar, *Multiply wound Polyakov loops at strong coupling*, *Phys. Rev.* **D 74** (2006) 026001 [hep-th/0603190] [INSPIRE].

[27] J. Gomis and F. Passerini, *Holographic Wilson loops*, *JHEP* **08** (2006) 074 [hep-th/0604007] [INSPIRE].

[28] J. Gomis and F. Passerini, *Wilson loops as D3-branes*, *JHEP* **01** (2007) 097 [hep-th/0612022] [INSPIRE].

[29] O. Aharony, J. Marsano, S. Minwalla, K. Papadodimas and M. Van Raamsdonk, *The Hagedorn-deconfinement phase transition in weakly coupled large-N gauge theories*, *Adv. Theor. Math. Phys.* **8** (2004) 603 [hep-th/0310285] [INSPIRE].

[30] L. Álvarez-Gaumé, C. Gomez, H. Liu and S. Wadia, *Finite temperature effective action,* AdS_5 *black holes and* $1/N$ *expansion*, *Phys. Rev.* **D 71** (2005) 124023 [hep-th/0502227] [INSPIRE].

[31] S. Sachdev and J.-W. Ye, *Gapless spin fluid ground state in a random, quantum Heisenberg magnet*, *Phys. Rev. Lett.* **70** (1993) 3339 [cond-mat/9212030] [INSPIRE].

[32] A. Kitaev, *A simple model of quantum holography*, talks at *KITP*, http://online.kitp.ucsb.edu/online/entangled15/kitaev, http://online.kitp.ucsb.edu/online/entangled15/kitaev2, University of California, Santa Barbara CA U.S.A., (2015).

[33] R. Dijkgraaf and C. Vafa, *Matrix models, topological strings and supersymmetric gauge theories*, *Nucl. Phys.* **B 644** (2002) 3 [hep-th/0206255] [INSPIRE].

[34] M. Hisakado, *Unitary matrix models and Painlevé III*, *Mod. Phys. Lett.* **A 11** (1996) 3001 [hep-th/9609214] [INSPIRE].

[35] C.A. Tracy and H. Widom, *Random unitary matrices, permutations and Painlevé*, *Commun. Math. Phys.* **207** (1999) 665 [math/9811154].

[36] *Digital Library of Mathematical Functions (DLMF) — eq.* (10.19.8), http://dlmf.nist.gov/10.19.

[37] *Digital Library of Mathematical Functions (DLMF) — eq.* (10.19.3), http://dlmf.nist.gov/10.19.

[38] J. Ambjørn, L. Chekhov, C.F. Kristjansen and Yu. Makeenko, *Matrix model calculations beyond the spherical limit*, *Nucl. Phys.* **B 404** (1993) 127 [*Erratum ibid.* **B 449** (1995) 681] [hep-th/9302014] [INSPIRE].

JHEP07(2017)030